Assessing risk for butterflies in the context of climate change, demographic uncertainty, and heterogenous data sources

Matthew L. Forister[1], Eliza M. Grames[1], Christopher A. Halsch[1], Kevin J. Burls[2], Cas F. Carroll[1], Katherine L. Bell[1], Joshua P. Jahner[3], Taylor Bradford[1], Jing Zhang[4], Qian Cong[5], Nick V. Grishin[4,6], Jeffrey Glassberg[7,8], Arthur M. Shapiro[9], Thomas V. Riecke[10]

[1] Ecology, Evolution and Conservation Biology, Department of Biology, University of Nevada, Reno, Nevada, USA

[2] Xerces Society for Invertebrate Conservation, Portland, Oregon, USA

[3] Department of Botany, University of Wyoming, Laramie, Wyoming, USA

[4] Howard Hughes Medical Institute, University of Texas Southwest Medical Center, Dallas, Texas, USA

[5] Institute for Protein Design and Department of Biochemistry, University of Washington, Seattle, Washington, USA

[6] Departments of Biophysics and Biochemistry, University of Texas Southwest Medical Center, Dallas, Texas, USA

[7] North American Butterfly Association, Morristown, New Jersey, USA

[8] Department of BioSciences, Rice University, Houston, Texas, USA

[9] Center for Population Biology, University of California, Davis, California, USA

[10] Swiss Ornithological Institute, CH-6204 Sempach, Switzerland

Correspondence: Matthew L. Forister, mforister@unr.edu

Open Research Statement: all data will be archived on Dryad upon acceptance for publication.

Abstract

Ongoing declines in insect populations have led to substantial concern and calls for conservation action. However, even for relatively well-studied groups, like butterflies, information relevant to species-specific status and risk is scattered across field guides, the scientific literature, and agency reports. Consequently, attention and resources have been spent on a miniscule fraction of insect diversity, including a few well-studied butterflies. Here we bring together heterogenous sources of information for 396 butterfly species and 1,004 subspecies to provide the first regional assessment of butterflies for the 11 western US states. For 184 species, we use monitoring and other observational data to characterize historical and projected trends in population abundance; for another 212 species (for which sufficient observational data are not available), we use exposure to climate change, development, geographic range, host breadth and other factors to rank species for conservation concern. We also organize information relevant to subspecific risk and prioritize a top 50 subspecies for further attention. A phylogenetic signal is apparent, with concentrations of declining and at-risk species in the families Lycaenidae and Hesperiidae. A geographic bias exists in that many species that lack monitoring data occur in more southern states where we expect that impacts of warming and drying trends will be most severe. Legal protection is relatively uncommon among the taxa with the highest risk values: of the top 100 species, one is listed as threatened under the US Endangered Species Act and one is a candidate for listing; of the top 50 subspecies, 15 have federal legal protection and one is under review for protected status. Among the many taxa not currently protected, we highlight a short list of species in decline, including *Vanessa annabella*, *Thorybes mexicanus*, *Euchloe ausonides*, and *Pholisora catullus*. Notably, many of these species have broad geographic ranges, which perhaps

highlights a new era of insect conservation in which small or fragmented ranges will not be the only red flags that attract conservation attention.

KEYWORDS

Anthropocene, butterfly, climate change, Lepidoptera, population viability analysis, demographic uncertainty, extinction, heterogeneous data, hierarchical Bayesian model

INTRODUCTION

Reductions in abundance, contractions in geographic range, extirpation, and extinction have become common features of wild plant and animal populations impacted by the various stressors of the Anthropocene (Dirzo et al. 2014, Turvey and Crees 2019). Effects on individual populations translate into depauperate assemblages of species in remaining natural lands, even those far removed from the most immediate effects of habitat destruction and degradation (McLaughlin et al. 2002, Brook et al. 2008). To the extent that the loss of evolutionary lineages (populations, species and higher taxonomic groups) is a part of life on earth and always has been, the current mass extinction crisis affords ecologists the chance to study extinction as an important earth-system process (Benton 2003). However, the need to maintain functioning natural ecosystems is increasingly generating motivation among scientists and the general public to reverse or slow whatever biotic losses might still be addressed (Naeem et al. 2016). Concern for functioning ecosystems has been elevated in recent years by a steady pulse of papers reporting declines in insect abundance and diversity (Eisenhauer et al. 2019, Wagner 2019) that have inspired calls for new conservation attention focused on "the little things that run the world" (Wilson 1987, Goulson 2019, Cardoso et al. 2020).

For certain charismatic and well-studied organisms, like the greater sage-grouse (*Centrocercus urophasianus*) or the desert tortoise (*Gopherus agassizii*), governmental agencies have been mobilized on a regional scale to monitor populations and management efforts, often in a proactive rather than reactive way (Pilliod et al. 2020). That kind of conservation and management depends on the synthesis of multiple lines of information including population monitoring, natural history studies, and geographic surveys. For insects, the taxonomic diversity is so great and the available information is so sparse (Cardoso et al. 2011), that proactive conservation informed by diverse data types has rarely been an option. As a consequence, insect conservation has often been motivated largely by fragmentation and small geographic ranges (Samways 2007, Diniz-Filho et al. 2010). Exceptions to that pattern include a few European countries where studies of butterflies have been sufficiently thorough in terms of natural history and monitoring that researchers have been able to prioritize species for conservation attention in a way that follows the International Union for Conservation of Nature (IUCN) and the Red List framework (Fox et al. 2011, van Swaay et al. 2011, Maes et al. 2012, Bonelli et al. 2018). That depth of species-specific information for insects is unusual, even for butterflies, and most countries will have a more complex mix of some monitoring or observational data, natural history observations, and expert opinion (New et al. 1995, Edge and Mecenero 2015, Geyle et al. 2021).

Butterflies in the western United States provide an excellent case study for the challenge of conservation prioritization that involves a mixture of heterogenous data types and sources of information. The region does include butterfly monitoring programs, but also expansive areas that are sparsely populated and understudied, including in particular the Intermountain West with hundreds of mountain ranges in the nearly 500k square kilometers of the Great Basin Desert. The

most temporally-intensive butterfly monitoring program in the western US is the Shapiro transect of ten permanent sites across Northern California that have been monitored biweekly during the flight season for between 35 and 51 years (Shapiro 2022). Many years before the entomological world made a collective pivot to the problem of insect declines (Hallmann et al. 2017), work with the Shapiro data documented shifting spring phenologies (Forister and Shapiro 2003), and the influence of land use and warming temperatures on extensive declines in abundance and species richness (Forister et al. 2010, Casner et al. 2014b).

Within the last couple of years, the issue has been raised of geographic and taxonomic heterogeneity or consistency of declines (Crossley et al. 2020, van Klink et al. 2020). This was the impetus for asking if results from the temporally-intensive Shapiro dataset would be consistent with geographically-extensive monitoring data from the North American Butterfly Association (NABA) and iNaturalist observations across the 11 western states (Forister et al. 2021). That effort quantified a compounding loss of 1.6% fewer butterflies observed per year and highlighted the negative influence of warming and drying conditions on butterfly populations in natural areas. However, the species included in Forister et al. (2021) were only those common and widespread enough to be present with sufficient frequency in monitoring databases to allow for inclusion in statistical models. Moreover, an attempt was not made to combine different lines of information into a ranking of species for conservation concern.

Here we address that need by taking a multi-faceted approach to conservation prioritization that utilizes observational data when available (for approximately half the species) and a combination of data types for other species, including natural history traits and quantitative estimates of exposure to climate change and development. We also include an assessment of subspecies using a combination of conventional conservation rankings and data on historical

occurrences. The different data types are detailed below and are used (1) to produce a quantitative ranking that highlights the taxa most severely declining and most likely to face regional extirpation or extinction in coming decades; and (2) to identify geographic and taxonomic knowledge gaps in our understanding of western butterflies. It is our hope that these results will be used by conservation practitioners and land managers to guide restoration and protection efforts, and will also motivate additional monitoring and the development of new population models that take maximum advantage of the heterogenous data types we have brought together. Throughout this paper, we use the word "risk" (and related terms, like "risk index") in a flexible way that encompasses evidence of past decline, projected declines, and combinations of traits that could predispose species to ongoing and future declines. This flexibility is necessary given the nature of our project encompassing species for which different kinds and quantities of information are available, but in all cases we intend the concept of high risk to flag species that could profitably receive careful attention from ecologists, conservation biologists, and the general public.

MATERIALS AND METHODS

A schematic overview of our methods is shown in Figure 1, emphasizing the flow of information from external data sources through analyses to the generation of quantitative risk assessment. All parts of the process are discussed in detail here. Starting with the 875 taxa on the North American Butterfly Association's 2nd edition checklist of butterflies occurring north of Mexico (NABA 2018), we retained 396 species with resident (non-vagrant) status in the eleven western states (Washington, Oregon, California, Idaho, Montana, Nevada, Wyoming, Colorado, Utah, New Mexico, and Arizona) based on range maps in Glassberg (2017), and collapsed 18

subspecies into full species. For clarity and in order to facilitate wide use of our results, we also reference a second checklist by Pelham (2022) in places where names differ. The Pelham list includes a larger number of subspecies and is thus important in particular for our organization of subspecific risk information, discussed in detail below.

Of the 396 species from the NABA list, 184 were present in monitoring databases (either the Shapiro transect or the NABA count circles) with sufficient frequency to be used in population models. For those species, which we will refer to in text and in figures as the "A group", our approach is to rank species based on observed and forecast population trajectories. Acknowledging the great uncertainty inherent to insect time series analyses, we present the ranking of A group species in a way that risk associated with other variables (e.g., geographic range size) can be evaluated by the reader. As will be discussed below, we use iNaturalist observations for A group species as a third source of historical information, but give it proportionally less weight than the Shapiro or NABA data.

For the other 212 species (the "B group", not present in monitoring schemes in sufficient frequency for inclusion in core population models), we have accumulated seven variables that form a composite picture of risk: geographic range, exposure to developed land, exposure to climate change, average (range-wide) precipitation, voltinism (number of generations per year), wingspan, and host breadth (or "host range"). We combine those seven variables into a single risk index as a weighted sum, where the weights are determined in part by our previous work with western butterflies, but also by analyses of the A group (described in detail below). The weighting scheme and other steps in data processing involve informed but partly subjective judgements with respect to threats to butterflies and natural history traits that predispose butterflies to risk. We have presented all data decisions in a transparent way, so that the reader

can judge for themselves the consequences of our methods and decisions, and alternative weights can be assigned by researchers using an online tool (see supplementary material). In the sections below, we describe first the three observational datasets (Shapiro, NABA, and iNaturalist) and associated analyses, then the seven other variables and how they are combined into composite risk indices and are visualized geographically and in a phylogenetic context.

North American Butterfly Association (NABA) counts and models

The NABA butterfly count program is a suite of hundreds of individual locations throughout the country that are monitored during midsummer (typically once, but in some cases more than once) by a group of at least four observers recording counts of all individual butterflies seen and identified to species, in a 15-mile (24.14 km) diameter circle. Observations from count circles in the 11 western states encompass different numbers of years at different sites from the 1970s to the present, with the final year in the dataset we examined being 2018 (the data were compiled for analysis in 2019). For the current project, we filtered the observations so that we only included sites that had been monitored for at least ten years, and with the final year being 2017 or 2018 (we did this so as not to generate forecasts for species with a substantial recent gap in observations). More than one monitoring day has been reported per year at a small number of sites, and for those locations we retained only the survey closest to the 4th of July, which is the traditional target date for these censuses. We then excluded any site-by-species combinations in which a species was not present for at least ten years (not necessarily consecutive years); finally, only species meeting the latter criterion for at least three locations were retained. Those filters resulted in a dataset with 162 species from 44 locations used in the core model and associated population forecasts (we experimented with less stringent filters but found that model

performance suffered). For species with less data, we ran a second set of models with lower thresholds, as described after the core model below.

Previous work with the NABA data used hierarchical Bayesian linear Poisson regressions run separately for each species (Forister et al. 2021). Here we advance that approach using a single, multi-species model that shares information about heterogeneity in the observation process across species observed at each site (Riecke et al. 2021). The components of the model (each described in turn below) include an observation sub-model, an abundance sub-model, and a forecast or simulation process that projects occupancy (the fraction of sites with non-zero presence by species) for various intervals of years in the future.

For the observational component, we modeled the counts of individual butterflies (y) using a Poisson distribution given the expected count of each species at each location during each year ($\mu_{\mathrm{t,l,s}}$), where t, l, and s identify the year, location, and species respectively:

$$y_{\mathrm{t,l,s}} \sim \mathrm{Poisson}\left(\mu_{\mathrm{t,l,s}}\right).$$

We modeled the expected count ($\mu_{\mathrm{t,l,s}}$) as a function of an abundance index ($N_{\mathrm{t,l,s}}$), year- and site-specific survey effort (β), and a year- and location-specific random effect ($\delta_{\mathrm{t,l}}$) shared among species:

$$\mu_{\mathrm{t,l,s}} = \exp(\ln(N_{\mathrm{t,l,s}}) + \beta * \mathrm{effort}_{\mathrm{t,l}} + \delta_{\mathrm{t,l}}),$$

with a vague prior for the effect of survey effort:

$$\beta \sim \mathrm{normal}(0,10).$$

The empirical variable for effort is the z-standardized total hours searched by all survey groups at a site on a day. After accounting for the effect of survey effort, we modeled additional variation in detection probability for each survey or monitoring day as a random effect shared among species. This random effect can be thought of as the combined effects of survey-specific

variation in detection due to processes such as variation in observer experience and local weather conditions (Riecke et al. 2021):

$$\delta_{\mathrm{t,l}} \sim \mathrm{normal}(0, \varsigma^2),$$

$$\varsigma \sim \mathrm{gamma}(1,1).$$

For the abundance sub-model, we assigned priors for initial population abundance indices for each species at their first encounter ($f_{\mathrm{site}_i,\mathrm{species}_i}$) at a study site as a function of initial survey effort and the initial count:

$$N_{\mathrm{f_{l,s}},\mathrm{l,s}} \sim \mathrm{gamma}(\exp[\ln(y_{\mathrm{f_{l,s}},\mathrm{l,s}}) + (\mathrm{effort}_{\mathrm{f_{l,s}},\mathrm{l,s}} * -0.1)], 1).$$

We modeled changes in population size (N) from one year to the next for each species at each site as a function of year (t), location (l), and a species(s)-specific population growth rate (λ):

$$N_{t+1,l,s} = N_{t,l,s} * \lambda_{t,l,s}\ .$$

Variation in population growth rate was in turn modeled as a function of a species-specific mean population growth rate (γ_s), and species-specific random variance in population growth rate:

$$\lambda_{t,l,s} \sim \mathrm{lognormal}(\gamma_s, \sigma_s^2),$$

$$\gamma_s \sim \mathrm{normal}(0,1),$$

$$\sigma_s^2 \sim \mathrm{gamma}(1,1).$$

Finally, for each species at each location, we projected the abundance index into the future using Monte Carlo simulation from the posterior distributions of species-specific population growth rate ($\lambda_{t,l,s}$), and species-specific population growth rate variance (σ_s^2):

$$N_{t+1,l,s} = N_{t,l,s} * \lambda_{t,l,s},$$

$$\lambda_{t,l,s} \sim \mathrm{lognormal}(\gamma_s, \sigma_s^2).$$

We defined local ‘extirpations’ as locations at which the expected count of a species given mean effort was less than 0.1 individuals, and calculated extirpation probability for each species at 10,

20, and 50 years into the future. Thus, one minus the extirpation probability is the probability of population persistence, and it is that value (probability of persistence) for each species from the core NABA model that moves forward (represented by 1k samples from the final year of the simulations) into the calculation of the risk index for the A group species.

The above model and 50-year projections were used for 162 species (in the A group) with sufficient data (passing filters described above). For another 105 species (with a median presence of 2 sites per species), we used a less complex model. These species are part of the B group with minimal observational data that were too sparse to be included in the core NABA model described above. However, in the interest of presenting maximal information on all species, we estimated trends through time for this subset of the B group (albeit at many fewer sites per species); the results are reported but not incorporated into the risk index calculation for these species. In this model, the counts (y) were also modeled with a Poisson distribution given the expected count for each location and year ($\mu_{\mathrm{t,l}}$), where t is the year and l is the location:

$$y_{\mathrm{t,l}} \sim \mathrm{Poisson}\left(\mu_{\mathrm{t,l}}\right).$$

The expected count ($\mu_{\mathrm{t,l}}$) was then modelled as a linear function of a site-specific intercept (α_{l}), a site-specific (s) year effect (β_1), and site-specific effect of effort (β_2):

$$\ln\left(\mu_{\mathrm{t,l}}\right) = \alpha_{\mathrm{l}} + \beta_{1,\mathrm{s}} * \mathrm{year}_{\mathrm{t}} + \beta_{2,\mathrm{s}} * \mathrm{effort}_{\mathrm{t,l}}.$$

The intercept and both beta coefficients were drawn from normal priors, with the normal truncated at zero to be positive for effort (β_2); the means and variances of those distributions were in turn drawn from hyperpriors (thus estimating effects across sites) with means drawn from normal distributions (with mean of zero and variance of 100) and variances drawn from gamma(1,1) as in the core model above. For 35 species present at only a single site, the model was run without the hierarchical (across sites) structure. The output of these secondary models

(for the 105 species) was retained as a directional probability (the fraction of the posterior distribution above zero for species with a positive year coefficient, and below zero for species with a negative year coefficient).

All Bayesian models were implemented using JAGS (version 4.3) and the `jagsUI` package (Kellner 2017) in R (R Core Team 2020). The core model (for A group species) was run with three chains for 500k iterations, with a 250k iteration burn-in. The secondary models (for the 105 B group species with some presence in the NABA data) were run with two chains for 2k steps and a 1k burn-in. Model diagnostics included inspection of plots of chain histories (all chains converged; $\hat{R} < 1.01$), and effective samples sizes.

Shapiro transect data and models

Ten long-term study sites across northern California have been monitored for between 35 and 51 years (depending on the site), with the presence of all butterflies noted along fixed routes every two weeks during the flight season. Data used here were compiled in 2021, including observations through 2020; earlier years were truncated so the dataset starts at 1985, except for three sites where data collection began in 1988. Species by site combinations of at least eight years were retained for analyses of 133 species. Additional details on sites, butterflies and field methods have been described elsewhere (Forister et al. 2010, Halsch et al. 2021, Shapiro 2022). In brief, data from the Shapiro sites have been analyzed using hierarchical Bayesian linear models in which the response variable (the number of days a species is observed in a year) is modeled as a binomial process, with a beta coefficient from the year term in the linear model representing change through time in the probability that a species is observed (Nice et al. 2014, Halsch et al. 2021). Here we use the version of this model and implementation as described in

Forister et al. (2021) in which the model was run separately for each species and beta coefficients for years are estimated within and across sites; the higher level coefficients (across sites) are used as indices of population change for each species across the northern California sites. As with the NABA models, model diagnostics included inspection of convergence and effective sample sizes. For downstream analyses (the creation of the risk index for A group species), 1k samples were retained from the posterior distributions of the year coefficients estimated across sites for each species. For two species, *Lycaena rubidus* and *Agraulis vanillae*, the year coefficients were extreme outliers (in the negative and positive direction, respectively) and were not used in the creation of the risk index values (described below) but we do include those coefficients in visual summaries of patterns across species.

The year coefficients from this modeling approach have been shown to be effective indices of change in total abundance as reflected in total counts of individuals which are available from a subset of years and sites (Casner et al. 2014a). Unlike the main NABA model, described in the previous section, we have not taken a forecasting approach with the Shapiro data. The two datasets have different strengths and weaknesses. The strengths of the Shapiro data are intensity and consistency of observation, which lend precision to estimates of species-specific change through time. In contrast, the NABA observations are only once per year, but the geographically distributed nature of the NABA sites (with greater independence among locations) lends value to the forecasting of population occupancy with our simulation approach (which does not account for dispersal or demographic connections among locations).

iNaturalist observations and expected ranges

Observations recorded on the iNaturalist platform are a wealth of geographic and phenological information, which researchers are increasingly using to answer ecological questions (Prudic et al. 2018, Kirchhoff et al. 2021), even for rare insects (Wilson et al. 2020). In our previous work with western butterflies, we used iNaturalist records in time series models, which revealed trends that were generally consistent with temporal patterns in the NABA and Shapiro data (Forister et al. 2021). Here we take a different approach, with the goal of using the broad geographic coverage of iNaturalist records to generate information on species status that is complementary to the detailed time series information from the other two observational datasets. We used iNaturalist records from the last 15 years (2007-2021) to generate a community scientist-derived estimate of area of occupancy. Those area of occupancy estimates were then compared to expert-derived range area estimates (described below) in a simple linear regression, and residuals from that relationship were saved. In other words, we asked which species have been seen more or less frequently in the last 15 years relative to the expected area based on the expert-derived range.

To generate the citizen scientist-derived area of occupancy estimates, we downloaded iNaturalist research grade observations from the Global Biodiversity Information Facility (GBIF.org 2021a, 2021b, 2021c, 2021d, 2021e, 2021f) for all butterfly species in the 11 western states. We retained observations from 2007 onwards for species that were observed at least 100 times (with very few exceptions, these were all A group species, present in Shapiro or NABA datasets, thus the analysis of iNaturalist records was confined to the A group). We calculated an unweighted Gaussian Kernel Density estimate using the function sp.kde from the R package `spatialEco` v1.3-7 (Evans and Ram 2021) based on the iNaturalist observations with a distance bandwidth of 2 (four examples are shown in Figure S1). The resulting raster was

converted to a disjoint spatial polygon (i.e. not all parts of the range needed to be connected) that encompassed all values > 0.00001 and calculated the area of the resulting range map.

Geographic ranges and voltinism

Expert-derived range estimates from Glassberg (2017) were generated from Keyhole Markup Language (.kml) files for each species. The range of each species was separated by voltinism (the number of generations per year in different portions of the range), with spatial polygons retained separately for uni-, bi-, and multivoltine regions. Quantitative areal estimates were then derived for all range portions within 11 western states using the area function in the R package `raster` v3.5-11(Hijmans et al. 2021), which estimates area based on the size of raster cells. This estimate is biased closer to the poles; however, we only generated range areas within the 11 western states (excluding portions of ranges that extended farther east, north into Canada, or south into Mexico) and thus the bias is expected to be minimal.

The expert-derived geographic ranges were used for multiple purposes (see Figure 1), including comparison with iNaturalist ranges (described in the previous section). The total expert-derived range estimates for each species were also used as a variable that contributes to the composite risk index, as did the fraction of the range that was univoltine (i.e., for simplicity, we focus on a univoltine vs bi- plus multivoltine comparison, rather than considering bivoltinism as a distinct category). The outlines of the expert-derived ranges were also used to calculate exposure to land use and climate (as described in the next section) and to calculate weighted latitudinal midpoints as another geographic descriptor. We used the function rasterToPoints from the `raster` package v3.5-11 (Hijmans et al. 2021) to convert each species range map to

coordinates; weighted latitudinal midpoints were then calculated that account for the longitudinal width of the range (i.e. the mean latitude across all cells in the raster).

As yet another line of expert-derived geographic information, we assigned each species a qualitative biogeographic designation of North, South, East, or West to reflect where the majority of the range area is found. For example, species labelled as western have the majority of their range in the 11 western states, with a minor presence north or south of the US borders or in the eastern states. Northern species have most of their range in Canada with only outlier (and often isolated) locations in the western US; similarly, southern species are those with ranges in Mexico often extending only dozens or hundreds of square kilometers into Arizona or New Mexico. Finally, species were labelled as eastern if they either had a transcontinental range (e.g., *Pieris rapae*, *Vanessa cardui*) or had a range almost entirely in the eastern states with only a minority of the range area in the 11 western states. These assignments were made by visual inspection of range maps in field guides (Scott 1986, Glassberg 2017).

Land use and climate change

Previous work with butterflies in our region has revealed effects of land use and climate change that are complex, potentially interacting, and dependent on both the species involved and the landscape context (Casner et al. 2014b, Forister et al. 2018, Halsch et al. 2021). Summarizing exposure to land use and climate change is not a simple task, but we have taken the relatively straightforward option of using the range outline (described in previous section) to quantify these stressors within the range of each species. Note that this differs from the use of point locations to quantify proximity to, for example, urban development (Jamwal et al. 2021). The range-outline approach is a better fit for our goals simply because all species have the same starting data (the

expert-derived ranges), which would not be true of 396 species using available point-occurrence records in, for example, iNaturalist. For highly mobile animals, like butterflies, the range-outline method has another advantage in that we do not have to assume that point locations of observations represent the only or most relevant habitats.

To quantify land use change, we reclassified the 2020 Cropland Data Layer (USDA 2020) into land cover types of agriculture, development, or natural and semi-natural habitats using the associated Cropland Data Layer scheme; all crops were classified as agriculture, development of any intensity level as development, and remaining land cover types (including pastureland) as natural or semi-natural habitat. For each species, we used the spatial polygon generated from the range map to clip the rasterized land cover types and calculated the proportion that was agriculture or development. This was done separately for regions of different voltinism, but these were summed to a single value for each species (see Figure S2 for examples of range-wide exposure to land use).

To estimate climate change exposure, we used TerraClimate data for minimum temperature, maximum temperature, and precipitation (Abatzoglou et al. 2018), which we resampled from ~4km spatial resolution to ~40km for computational efficiency. Using multivariate Mahalanobis distance as a measure of departure (Farber and Kadmon 2003, Abatzoglou et al. 2020), we calculated departure from baseline conditions (1958-1987) for the most recent thirty years (1991-2020) for each cell. To estimate exposure to climate change, we calculated rate of change in departure over time using Theil-Sen slopes (Theil 1950, Sen 1968) which estimate the median slope between each pairwise set of observations and are relatively robust to outliers near the start or end of a series. We generated a raster of these trends in departures for the eleven western states. For each species, we then clipped the climate departure

raster layer using the species range maps as spatial polygons and calculated the mean climate change exposure across that portion of the range (as with land use, this was done separately by voltinism, but then added for a single value per species for further analyses; see Figure S2 for examples). We also calculated 30-year climate normals (1991-2020) for minimum temperature, maximum temperature, and precipitation annually and within each season across the entire range for each species. Among those three variables, precipitation was recently found to be predictive of changes in butterfly abundance across the west (Forister et al. 2021), thus it was used as a static description of climate for inclusion in the composite risk index (described below).

Wingspan and host range

Among the many morphological and natural history traits that could be informative of status and risk, body size and ecological specialization are widely studied, and thus relevant data are available for many species. More narrow diets are often associated with greater sensitivity to habitat loss and other disturbance (Hughes et al. 2000), and dispersal ability is a key determinant of metapopulation resilience in the face of fragmentation or other stressors. Wingspan has been shown to be a proxy for dispersal ability in butterflies (Sekar 2012). For most of the butterflies studied here, wingspan was previously estimated (in Forister et al. 2021) with data derived from Opler (1999). For a small number of species included in the present study for which a measurement was not available from that source, we supplemented with ad hoc online searches. Similarly with diet breadth (or host range), we used a single source for the vast majority of species (Scott 1986), and supplemented from other field guides and other online resources for the few species with missing data.

We gathered both the number of plant genera and plant families reported as caterpillar hosts for each species, and then calculated a combined index of diet breadth as the number of taxonomic families plus the natural log of the number of genera. That calculation of taxonomic diet breadth puts most weight on the number of families but allows for some influence of the number of genera eaten. For example: a species that uses hosts in two genera in two families would have a diet breadth of 2.69 (2 + ln(2)), while a species that uses plants in three genera in two families would have a diet breadth of 3.10 (2 + ln(3)). We did not attempt to gather species-level host records, for which too much data would be missing or unreliable.

Transformations

In total, we compiled ten variables that contribute to the prioritization of A and B group species in different ways: (1) 50-year occupancy projections (probabilities of population persistence) based on NABA data; (2) historical rates of change from the Shapiro data; (3) recent change in range based on the difference between community scientist-derived and expert-derived ranges; (4) geographic range based on expert assessment; (5) exposure to agricultural and other developed lands; (6) exposure to climate change; (7) average precipitation throughout the range; (8) the fraction of the range with one generation per year; (9) wingspan; and (10) an index of diet or host breadth (Figure 1). Prior to their use in assigning a risk value to each species (discussed in the next section), each variable was subjected to a specific set of transformations that resulted in a variable with a range of 0 to 1 where larger values represent greater risk. Depending on the nature of the variable (when larger values do or do not naturally represent higher risk), the transformations included inversion, and (for all variables) standardization between 0 and 1 (by dividing by the largest value). In some cases, for highly skewed variables, a natural log

transformation was applied as the first step. For example, wingspan was first log transformed, then multiplied by -1, such that all values become negative and the larger wingspans become larger negative numbers; the distribution was then shifted to the positive by adding the absolute value of the smallest (most negative) value to all of the numbers; finally, the distribution was divided by the largest value, thus scaling the numbers between 0 and 1, where the smallest wingspans (representing the greatest risk because of less dispersal ability) are now closest to 1. All transformations and scaling steps are illustrated in Figure S3.

For visualization of the transformed and scaled variables, we divided the distributions (Figure S3) into quantiles and assigned circles of different sizes to the different intervals, with larger circles indicating larger values and greater assumed risk. For most of the variables, we found that the following breakpoints provided a useful assignment of circles for visualization: 0.15, 0.5, and 0.85; in other words, the interval from 0 to 0.15 was assigned the smallest circle (the least risk), from 0.15 to 0.5 the next largest, etc. Breakpoints differed for some of the more skewed variables (e.g., host range), but the results are interpreted in the same way (larger circles represent larger assumed risk).

Calculation of risk index for A and B group species

The A group species are those species for which data were available from at least one of the monitoring programs (Shapiro or NABA), and many of these species also had enough iNaturalist observations for analysis. For these species, we calculated a weighted sum based on those three lines of information with weights as follows: 47.5% NABA, 47.5% Shapiro, and 5% iNaturalist. The small weight given to the iNaturalist data reflects the fact that the data are heterogeneous (in space and among species) and rapidly accumulating; these data are thus complex and potentially

important but still only barely explored from an analytical perspective. Alternative weighting schemes among all variables (including the three observational variables) can be explored using an interactive, online tool; see supplementary material.

The variables used in our A group weighting scheme (multiplied by the three percentages, 47.5%, 47.5%, and 5%) were the 50-year probabilities of persistence (from NABA), historical rates of change (from Shapiro), and observed range changes (from iNaturalist) that had been transformed (see previous section) such that larger values represent greater evidence for decline or (in the case of NABA) projected decline. Thus, a species with the most severe declining values (historical or projected) for each dataset would receive a composite risk score of 1. To incorporate uncertainty retained from Bayesian analyses of the NABA and Shapiro data, the composite risk index was recalculated 1k times using 1k samples of the relevant posterior distributions; we then calculated a mean and 85% highest density interval of risk for each species.

The B group species are those lacking observational data. Thus, we used a composite of the other seven variables to estimate risk. We experimented with a number of weighting schemes for those seven variables and settled on an approach that was partly influenced by previous research (e.g., Forister et al. 2021) but also informed by an additional analysis of the species in the monitoring data. Specifically (for that additional analysis), we took the composite risk index for the A group species (based on NABA, Shapiro, and iNaturalist data) and used linear regression models to determine which of the other seven variables were most predictive of that risk index (following general protocols with other Bayesian models as described above). The exact weighting scheme for B group species (influenced partly by results of the analysis of the A group) is described fully in results below. Clearly many schemes are possible for a weighted sum

of seven variables, and we report correlations among outcomes from different schemes. Finally, many of the B group species had some data from the NABA dataset that were not sufficient for inclusion in our main model and occupancy forecasts. For those species, we ran a less complex model (described above as the secondary set of NABA models) and report the results along with other B group results, but we do not incorporate those values into the B group risk index to maintain consistency in risk index calculations.

The calculation of the risk index for both the A and B groups relied on a complete data matrix. For most of the variables used for the B group, there were no missing values, specifically for all of the variables deriving in part from the expert geographic ranges: range area, voltinism, precipitation, development, and climate departure (Figure 1). A few species lacked data for host range, and these we filled with interpolation of the median value calculated across all species. A more consequential decision was to similarly use median interpolation with the observation data and the A group species. In other words, a species without sufficient iNaturalist observations for analysis was given the median value associated with that variable prior to the calculation of the risk index. The same was true for species not represented in the NABA or Shapiro data: lacking any other information we assume those species are simply following the central tendency (for historical and projected change) as estimated across other species.

Risk index for subspecies

A list of subspecies present in the western United States (Arizona, California, Colorado, Idaho, Montana, New Mexico, Nevada, Oregon, Utah, Washington, and Wyoming) was gathered from Pelham (2022). Geographic inclusion for subspecies was based on described ranges in original descriptions and records from public databases (n = 1,004 subspecies). Two categories of

502 conservation need were considered in ranking subspecies: 1) global, national, and subnational
503 (state) ranks assigned by the organization NatureServe; and 2) the last year a subspecies had a
504 publicly available recorded observation based on our inspection of available databases.

505 A full description of NatureServe ranking methods and rank descriptions is available in
506 Faber-Langendoen et al. (2012). Briefly, ranks are assigned a 1-5 number where 1 is Critically
507 Imperiled, 2 is Imperiled, 3 is Vulnerable, 4 is Apparently Secure, and 5 is Secure. Rankings are
508 assessed using a Rank Calculator that includes aspects of rarity, threats, and population trends.
509 Ranks are used to assess imperilment over the entire (global) range of subspecies as well as at
510 the national and state levels. For subspecies, global rankings are indicated by a “T” rank
511 following the global rank. Thus, an Imperiled subspecies (rank of 2) of an Apparently Secure
512 species (rank of 4) would have the rank G4T2. National (“N”) and state (“S”) rankings are
513 assessed separately for species and subspecies. Additional ranks are “X” for taxa that are
514 presumed extirpated, “H” if a taxon is possibly extirpated with records in the last 20-40 years
515 and might be rediscovered, as well as others including "NR" for taxa that have not yet been
516 assessed (Faber-Langendoen et al. 2012).

517 First, we created a summary measure of subspecies imperilment at various geographic
518 scales based on the NatureServe evaluations by creating a quantitative scale for global, national,
519 and state rankings. Points increased with imperilment, such that a rank of G1 is worth 4 points
520 and G5 is worth 0 points. This scoring was completed similarly for the nominate species global
521 ("G") ranks, global subspecies (“T”) ranks, national (“N”) ranks, and each state with a S1-S5
522 ranking. State scores for each species were averaged to create a single state-level score. Any
523 other rankings including "X" and "H" were scored as a 0 as these are equally uninformative with

respect to realized conservation need. A total score for each taxon was calculated as the sum of the global, national, and state scores such that a taxon could have a score from 0-16.

Second, the most recent year of observation for each subspecies was collected from various accessible databases, websites, photographic collections, and peer-reviewed literature, with a goal of finding one observation for a taxon from 2001 or more recent as evidence of recent presence. Searches began with all specimen records by family in the Symbiota Collections of Arthropods Network for the 11 western states (SCAN 2022). For any taxon that did not have a post-2001 observation, progressive searches through the literature were made until one was found or until all references had been searched for the most recent record available; a full list of resources used is available Table S1. Any taxon with a record from 2001 or more recent received a score of 0, and each year previous to this increased the score by 1 point. Scores for this category ranged from 0 to 34 (for *Megathymus yuccae harbisoni*). While we have done our best to collect available observations, identification to the subspecies level was challenging at times due to either recent taxonomic changes or difficulty identifying individuals using only photographs. We do not believe these issues significantly affect our overall ranking of subspecies.

As with the species-level risk assessment, subspecies values for each of the three categories were normalized to be between 0 and 1 before the calculation of a composite index. The NatureServe score was given 75% weight towards a total score as it includes the most information regarding total threat or risk, and the year of observation scores were given 25% weight. Weighted scores for the two categories were added together to create a single comprehensive score for each subspecies between 0 and 1. Those scores were used to rank the subspecies, and we also asked if subspecies risk values were correlated with risk calculated

independently at the species level (calculations described in previous section). For species with multiple subspecies evaluated for risk, the subspecies values were averaged (within each nominal taxon), and then a simple Pearson correlation was calculated between the two sets of risk values (at the species and subspecies level).

Geographic and Phylogenetic visualization of risk

Finally, we asked how the composite risk indices were distributed across the landscape and across the phylogeny of western butterflies. From a spatial perspective, we calculated both species richness (separately for each cell in a raster covering the extent of the eleven western states) and average risk among species present in a cell. We did this separately for the A and B group species, and we restricted analyses to only species with higher risk values by subsetting to the upper 75th quantile of risk values separately for each list (A and B). Within those higher-risk groups, we converted each species range map from a spatial polygon to a raster layer where values within the range were set to 1 and values outside the range to 0. We summed these values across all rasters to produce a new raster of species richness. To calculate mean risk for each cell, we divided the cumulative risk index raster by the species richness raster.

For the evolutionary perspective, we used the phylogeny from Zhang et al. (2019) for all 845 butterfly species from the United States and Canada. Briefly, this tree was based on 756 universal single-copy orthologs we identified from 36 reference genomes using `OrthoMCL` (Li et al. 2003). Sequences of these orthologs were aligned using both local (BLAST [Altschul et al. 1997]) and global (MAFFT [Katoh et al. 2002]) alignment methods, and only positions that were consistently aligned by both methods were used. Sequences of non-reference species were derived by mapping the Illumina reads to the exon sequences of the reference species and

performing reference-guided assembly. Multiple sequence alignments (MSA) of different orthologs were concatenated to a single MSA. This MSA was partitioned by codon position and used to build a tree by `IQ-TREE` (version 1.6.12) (Nguyen et al. 2015) with the most suited evolutionary model automatically found by `IQ-TREE`.

The phylogeny was imported as a time-calibrated .tre file into R and pruned to our focal western butterflies (the combined A and B group lists). The package `ggtree` (Yu et al. 2017) was used to plot a phylogeny with tips labelled by risk categories assigned based on the quantiles of the risk distributions separately for the A and B group species. Specifically, species in the upper 90th quantile were labelled as "high risk," species between the 75th and 90th quantiles were labelled as "medium risk", and species below the 75th were "low risk." Finally, the phylosig function from `phytools` (Revell 2012) was used to calculate lambda and K (with 1000 simulations for the permutation test) as measures of phylogenetic signal for the continuous risk index across all species, which in this context is informative with respect to the extent to which closely related species share similar levels of risk.

RESULTS

We calculated an index of risk for 396 species, which includes two groups: 184 species in the A group with extensive monitoring or observational data, and 212 species in the B group without observational data (or without enough to be used in our primary population models). Not surprisingly, the B group species tend to have smaller geographic ranges (Figure 2a), which in part explains their reduced presence (just by geographic chance) in monitoring groups, but the two groups differ in other ways (Figure 2). The B group species have slightly lower exposure to development (Figure 2b) and moderately higher exposure to climate change (Figure 2c). The

593 higher climate change exposure is explained in part by the greater presence of more southern
594 species in the B group, as seen by latitudinal midpoints (Figure 2g) and qualitative
595 characterization of range (Figure 2h).

596 For the A group species, we modeled historical and projected population trajectories
597 using different sources of observational data. Consistent with previous work with NABA data,
598 our new model with shared (across-species) observation heterogeneity found a majority of
599 species (71%) with annual growth rates below replacement (Figure S4). We used those estimated
600 annual growth rates and the most recent year of observed counts to simulate 50 years into the
601 future. The median fraction of extant locations (or probability of local persistence) per species at
602 50 years was 0.60, and that fraction was positively related to historical population growth rates
603 (Figure S4). Results from analyses of Shapiro data also find a majority of species with downward
604 trends through time of varying magnitude (84.5% of species have negative year coefficients). We
605 combined the 50-year persistence estimates (from the NABA model) with historical rates of
606 change (from the Shapiro data) and an estimate of shift in range size based on community
607 scientist observations (from iNaturalist) relative to expert range sizes to generate a composite
608 risk index for the A group species. Note that the A group species are shown in Figure 3 with risk
609 information associated with the other seven variables (geographic range, exposure to
610 development, etc.), even though the actual ranking of the A group is based solely on the
611 observational data (NABA, Shapiro, iNaturalist). We present the information in this way because
612 we acknowledge the imperfect geographic coverage of monitoring programs and the inherent
613 uncertainty in population models. Thus, the reader or conservation practitioner can easily see if
614 two species with similar risk values in the A group (based on NABA, Shapiro and iNaturalist
615 results) potentially have similar risk based on other variables like range size. We also generated

the risk values with an even split in weights between NABA and Shapiro data (leaving out iNaturalist), and found that the resulting risk values were correlated with our primary risk values at $r = 0.997$ (which reflects primarily the low weight assigned to iNaturalist observations but also the fact that they are correlated with results from Shapiro data, Figure S5).

Without observational data, the ranking of B group species required a partitioning of weights among the other lines of information. To partly inform that process, we used the A group species to estimate the effects of other variables on risk index (based on NABA, Shapiro, and iNaturalist data). The model explained a relatively small proportion of variance in the risk index (Table S2), but did demonstrate that smaller wingspans (99% probability of effect) and lower range-wide precipitation (86% probability of effect) are associated with risk for the A group species. In addition, we also suspected climate change would be important based on our previous work with western butterflies (Forister et al. 2021, Halsch et al. 2021). This is especially true given the large presence of B group species with ranges in the desert southwest (Figure 2h), a region heavily impacted by warming and drying trends. We adopted the following weighting scheme to calculate a single risk value for each species in the B group: 20% precipitation, 20% wingspan, 20% climate change, 10% development, 10% range size, 10% voltinism, and 10% host range; correlations among the seven variables as well as the three observational variables (for the A group) are shown in Figure S5. As a comparison to that scheme, we also ranked the B group species with equal weights among the seven variables (14.3%); the resulting risk values were correlated at $r = 0.90$ ($t = 29.32$, df = 210, $P < 0.001$) with the values from the primary scheme. With a third weighting scheme based on 50% from each of average range-wide precipitation and wingspan (the two variables identified by the analyses of A group risk), the correlation with the main scheme was $r = 0.55$ ($t = 9.66$, df = 210, $P < 0.001$).

The top fifty species with the highest risk values from each of the A and B groups are shown in Figure 3 (the other species with lower risk values are in Figures S6, S7 and S8). For the highest-ranked A group species, agreement between the two monitoring schemes is apparent with large "risk circles" in both the NABA and Shapiro columns (Figure 3a). In some cases, these top-ranked A group species have also been seen less frequently over the last 15 years relative to expectation based on the expert-derived range maps (see the iNaturalist column in Figure 3a). Time series plots for two of those top species are shown in Figure 4 (*Vanessa annabella*) and Figure 5 (*Euchloe ausonides*); in Figure 6, neutral or upward trajectories can be seen for *Poanes melane*, the species with the lowest risk index among the A group species (Figure S8). Similar plots for all other A group species are available through an online tool (see supplementary material). The rankings for the A group species are shown with 85% credible intervals (Figure 2a), which are broad; this uncertainty reflects the high inter-annual variability inherent to the time series data being modelled (from both NABA and Shapiro) and should be kept in mind when interpreting the position of species on the A group list.

We compiled data for 1,004 subspecies, and ranked them using criteria that were largely based on NatureServe ratings, but also included the last year in which an observation was reported for a particular taxon. The 50 subspecies with the highest priority for conservation are shown in Table 1, where the high frequency of butterflies in the family Lycaenidae is notable, with almost half (22 out of 50) in the top 50 list in that family. Another 15 taxa are in the Nymphalidae family, 8 of which are subspecies of *Speyeria* [*Argynnis*], a charismatic group of subspecifically diverse species. It is interesting to note that the split between A and B group species in the top 50 subspecies list is 31 A group and 19 B group, which at least suggests that the evaluation of subspecies is not necessarily biased towards species with the smallest ranges

662 (which tend to be the B group species; Figure 2a). Additional information on the 1,004
663 subspecies that we evaluated is available in archived data for this project (see data availability
664 statement), and in an online tool where output similar to Table 1 can be filtered by state and by
665 family (see supplementary material).

666 We also asked if the risk index calculated at the subspecies level could be predicted by
667 the risk index calculated at the species level (Figure 3). An overall correlation was detected
668 between the two indices at $r = 0.17$ (t = 2.05, df = 140, $P = 0.04$), and the relationship was driven
669 by the B group species. With the data split into the A and B groups, a correlation was not
670 detected for the former ($r = 0.10$, t = 0.95, df = 99, $P = 0.34$) but was for the latter: for the
671 species without monitoring data (the B group) the risk index calculated at the species level is
672 correlated at $r = 0.28$ (t = 2.15, df = 55, $P = 0.0036$) with the risk index at the subspecies level.

673 Finally, we examined the distribution of the species-level risk index geographically and
674 phylogenetically. Considering the species with the highest risk index values (above the 75th
675 quantile of risk values) for the A group, across the 11 western states the spread of average risk
676 shows a partially inverted relationship with richness of the most at-risk species in some parts of
677 the region (Figure 7). For example, average risk is high in the northern Central Valley of
678 California and in the northwestern region of Oregon (Figure 7a), while total richness of at-risk
679 species is lower in those areas (Figure 7b). Similarly, richness of at-risk species is high in the
680 Sierra Nevada, but average risk is low. The distributions of risk for the B group species highlight
681 the bias of that group towards the most southern areas, with high average risk along the southern
682 California coast (Figure 7c) and a concentration of at-risk species along the border between
683 Mexico and New Mexico (Figure 7d).

The phylogenetic picture of risk shows multiple clusters of at-risk species, and some lineages with notably lower risk, like the Papilionidae and much of the Nymphalidae (Figure 8). The families sharing the disproportionate amount of risk are the Hesperiidae (with 16% of species in the high risk category, above the 90th quantile of risk) and the Lycaenidae (with 14% of species at high risk); these are followed by the Riodinidae (with 13% of species at high risk, albeit based on a small sample size with the family represented by only 8 species) and the Pieridae (with 12% of species at high risk). The percentages of high risk species in the Papilionidae and Nymphalidae are just 8% and 1%, respectively (Figure 8). Tests of phylogenetic inertia are consistent with the observation of phylogenetically clustered risk (Pagel's $\boldsymbol{\lambda} = 0.39$, $P < 0.001$; Blomberg's $K = 0.052$, $P = 0.001$ based on 1k randomizations).

DISCUSSION

Our primary goal in this paper has not been to document butterfly declines or to identify traits that make insects more or less sensitive to the stressors of the Anthropocene, as these topics have been addressed elsewhere for North America (Schultz et al. 2019, Wepprich et al. 2019, Crossley et al. 2021, Forister et al. 2021), the Neotropics (Janzen and Hallwachs 2019, Salcido et al. 2020), and numerous other parts of the world (Nakamura 2011, Fox 2013, Wagner 2019). Instead, our goal has been to organize and analyze heterogenous data sources in a way that allows conservation biologists to identify the butterflies in the 11 western US states that are most likely to suffer serious reductions in range or population size in coming years. We hope that our work advances the issue of the prioritizing of species for conservation given mixed data types, uneven spatial coverage and uncertainty in historical trends. Although some parts of the world

706 (notably countries in western Europe) have dense coverage with standardized monitoring,
707 prioritization in most of the world will involve some mix of monitoring and trait-based inference.
708 The western states have been our region of study, rather than the entire US, because the
709 impacts of climate change are severe and distinct in this arid region (Gonzalez et al. 2018), and
710 the butterfly fauna is similarly shaped by a unique topography and climatic history (Shapiro
711 1996, Hawkins 2010). At the continental scale, butterflies in the west also appear to be
712 experiencing the most severe declines (Crossley et al. 2021). As a consequence of expansive
713 areas with low human population density, about half of the butterfly species in the region are not
714 included in the monitoring datasets used here, yet we have brought together information on the
715 entire fauna (with the exception of a few species with rare occurrences, mostly strays across the
716 US-Mexico border). Because of this, our study has an apples-and-oranges structure (species with
717 and without monitoring data) that extends to the interpretation of the risk index values and
718 engenders certain ironies. Chief among the ironies of our work is the fact that we rank B group
719 species in part by certain variables (geographic range, exposure to climate change, etc.) that are
720 not evidently associated with declines in the species for which we have historical records (the A
721 group). In other words, considering Figure 3, the A group species near the top of the list do not
722 necessarily have the smallest ranges, and the same can be said of other variables. Even for the
723 two variables (wingspan and average precipitation) which do predict risk in the A group, the
724 variance explained is low (Table S2) yet we still emphasize these variables in ranking the B
725 group species. We discuss these apparently counterintuitive decisions below, and then discuss
726 phylogenetic and geographic hotspots of risk. Finally, we end with a consideration of individual
727 taxa most deserving of attention given available evidence.

728 Among the complexities of variables potentially associated with risk, an understanding of
729 geographic range starts by noting that the A group species have broader geographic ranges
730 (Figure 2a), which is indeed why they are present at enough NABA sites to be included in our
731 core population model. Thus the fact that many of the most severely declining species are
732 widespread (e.g., *Vanessa annabella* in all 11 states) does not diminish the logic of prioritizing B
733 group species based in part on small range size, which is a well-known determinant of risk
734 (Staude et al. 2020). Similarly, the effects of voltinism and ecological host specialization are
735 relatively straightforward: everything else being equal, we expect a species with multiple
736 generations per year and an ability to utilize many hosts to be more resilient (to any number of
737 stressors) than another species without those traits (Eskildsen et al. 2015).

738 The interpretation of other variables is less straightforward, chief among them being
739 exposure to climate change. Previous work with western butterflies has identified warming and
740 drying conditions as stressors, based in particular on analyses of geographic variation among
741 study sites in climate change effects and changes in aggregate butterfly density (Forister et al.
742 2021). At the species level (rather than the level of individual study sites), the same signal is not
743 as apparent in the present study for the A group species (in other words, the species towards the
744 top of the A group list do not have particularly high exposures to climate change). This is
745 because most of these species have large enough ranges that their exposure to climate change
746 (when quantified across the entire range) includes areas with both more and less severe warming
747 and drying that tend to cancel each other out at the scale of broadly-distributed species.
748 However, the B group species have smaller and more southern ranges (Figure 2), which is the
749 part of the west most impacted by climate change (Gonzalez et al. 2018). Thus, we believe

750 exposure to climate change is well justified as a contributing factor to risk specifically for these
751 species for which we lack monitoring data.

752 Exposure to development (urban, suburban and agricultural lands) requires similarly
753 careful interpretation. This is chiefly because the data most well suited to understanding the
754 effects of habitat destruction on insects will rarely be collected: places that have already been
755 developed will not be monitored, and existing monitoring efforts will often be located in more
756 pristine locations even when relatively proximate to human habitation. The Shapiro dataset is an
757 exception, as it encompasses a severe land use gradient from the agricultural and urban Central
758 Valley to the undeveloped high elevations of the Sierra Nevada. From that program, we know
759 that land conversion and contamination (with pesticides) have effects of similar magnitude at
760 low elevations (Forister et al. 2016). Though similar information does not exist across the west,
761 we included exposure to development in our rankings here for the B group species for the simple
762 reason that common sense suggests that a range that encompasses more development is likely to
763 experience increasing fragmentation and contamination in coming years relative to a species with
764 less exposure.

765 Geographic projections of risk for B group species emphasize the southern areas of the
766 west (Figure 7), but also point to specific hotpots of average risk that include the southern
767 California coast. Like A group species in the Central Valley of California, that coastal region has
768 low richness of B group species, but on average the species that are there in the vicinity of the
769 Los Angeles basin score high for our risk factors. Arizona and southwestern New Mexico have a
770 high concentration of B group species with high risk factors, thus this area should be prioritized
771 for future monitoring efforts. For A group species, the Sierra Nevada Mountains (especially the
772 northern Sierra), the Colorado Plateau and the southern Rocky Mountains are hotspots of

declining species (Figure 7). These same places have been recently identified as hotspots of imperiled species in analyses that included plants, vertebrates, freshwater invertebrates and some terrestrial insects (Hamilton et al. 2022). For both A and B group species, iNaturalist records (and other distributed, community-scientist platforms such as eButterfly) hold great promise for understanding population trajectories in coming years.

We have used iNaturalist records to ask if species have been seen across smaller or larger areas relative to expectation based on the areal extent of expert derived range estimates. We consider that approach to be exploratory and gave it a corresponding low weight in our ranking. Although we used research grade observations from iNaturalist (Hochmair et al. 2020), misidentifications are still possible and (more generally) complexities in taxonomic usage and metadata associated with GBIF (the Global Biodiversity Information Facility from which we accessed the records) produce challenges when merging with other datasets. We have been conservative in our vetting of that process but acknowledge that tool development in this area is needed, and we offer our results in the hope of encouraging other researchers to explore creative uses of iNaturalist and other publicly-sourced records. Despite the potential issues, we note that the variable for change in range size that we derived from the iNaturalist-to-expert comparison was positively correlated ($r = 0.21$) with historical trajectories derived from Shapiro data (Figure S5) but not with 50-year projections based on NABA data ($r = 0.04$).

Phylogenetically, risk values are strongly clustered within and among families, with notable concentrations in the Lycaenidae and Hesperiidae, with the latter in part due to both species with small southern ranges (B group species) and species in monitoring programs with observed declines. Of the high-risk category species (with risk index values above the 90th quantile), 53% are Hesperiidae. The family Nymphalidae has the lowest concentration of at-risk

species, although one of the most notably-declining species is in this family. Despite being large and dispersive and able to use a number of exotic plants as larval hosts, *Vanessa annabella* is becoming hard to find across locations that include urban centers, high mountains, and southern deserts (Figure 4).

Although *V. annabella* is deservedly at the top of the risk list (Figures 3 - 4), we stress the uncertainty in the actual risk values that we have generated and we do not place much weight on the exact position of species on that list. In other words, we believe that the top species in the A group are indeed in historical declines that will likely continue in coming years, but the fact that one species is in the 4th position vs the 10th or even the 25th position on the list is not necessarily important. Small differences in, for example, the projected 50-year probability of population persistence affect the positions for those top species which have mostly similar risk values (and broadly overlapping credible intervals). This is why we conservatively suggest that all of the top 50 species in the A group (Figure 3) deserve closer scrutiny and in some cases likely deserve protection. The fact that rankings should be treated as approximate is also why we have presented other lines of information (geographic range, host specialization, etc.) for the A group, even though the risk index ranking is based solely on the observational data (NABA, Shapiro and iNaturalist) for those species. For example, *Pontia protodice* and *Lycaena xanthoides* have nearly identical risk indices, but the latter (*L. xanthoides*) is univoltine with a smaller geographic range, greater exposure to development and a more specialized diet (Figure 3); these are all factors that could be considered by conservation biologists and ecologists interested in declining insects. With respect to current protections, only two of the species that we have studied have status at the federal level: one of the A group species (the monarch butterfly, *Danaus plexippus*) is currently a candidate for protection under the US Endangered

819 Species Act (ESA), and one of the B group species, *Lycaena hermes*, is currently listed as
820 threatened. Note that *Boloria acrocnema* is treated as a full species under the ESA, but we have
821 followed both NABA (2018) and Pelham (2022) in counting it among the protected subspecies
822 (*Boloria improba acrocnema*) in Table 1.

823 Our presentation of the top 50 species in the A group (Figure 3) includes sample sizes
824 (for NABA and Shapiro datasets) which should also be considered when judging the evidence
825 for risk. For example, the 2nd and 3rd species on the A group list (Figure 3) are represented by
826 data from 3 or fewer sites for the NABA and Shapiro datasets, and are not represented in
827 iNaturalist analyses. The small samples for those species are reflected in broad intervals around
828 the risk values, and it can be noted that other species in the top 10 for the A list are known to be
829 in decline based on evidence from two to three times as many sites (e.g., *Pholisora catullus*,
830 *Atalopedes campestris*, and *Euchloe ausonides*). The number of sites for individual species is a
831 reflection not just of information available for analysis, but it should be remembered that risk
832 associated with the NABA data derives from a multi-species population viability analysis, and
833 species with fewer sites are more likely by chance to have lower occupancy in forecasts than
834 species known from a greater number of sites. This is both a methodological feature of stochastic
835 simulations but also reflects a biological reality in that more widespread species are known from
836 a greater number of NABA sites (thus geographic range is indirectly involved in the contribution
837 that the NABA analyses make to our estimate of risk).

838 Yet another important aspect of sample size involves the great many A group species not
839 represented in all three of the observational datasets (Shapiro, NABA and iNaturalist); for these
840 species, we used median interpolation. In other words, when calculating the risk index for a
841 species present in, for example, the Shapiro and iNaturalist datasets but not NABA, we assigned

a 50-year projection value based on the median across all other species represented in the NABA dataset. For the present effort, we consider this to be at least a relatively simple assumption, although we acknowledge that future analyses could use more sophisticated interpolation perhaps including information from closely related species. The phylogenetic signal observed here suggests that genetic relatedness could be a tool for dealing with uncertainty and missing data in conservation ranking.

The weight of missing data and uncertainty of course becomes greater when we turn to the top 50 species in the B group (Figure 3) for which monitoring data is either absent or insufficient for robust models. Not only is robust observational data lacking, but so many of the B group species are similar in having small ranges in hot and dry parts of the region that the overall spread of risk values is smaller than for the A group. Thus, rankings in the top 50 for the B group should be taken with an even more substantial serving of salt. Indeed, there are certainly species beyond the top 50 that merit careful scrutiny. For example, *Strymon avalona* is restricted entirely to Catalina Island (less than 200 square kilometers) off the coast of southern California. The partly wild nature of the island gives the species a low development score and the area happens to be characterized by only moderate departure from climatic baseline. Thus *S. avalona* ranks outside of the top 50 for the B group (Figure S6), even though that small geographic range of course puts it at risk of stochastic loss. Similarly, many of the B group species below the top 50 have red lambda symbols (to the right of the panel) which indicate negative annual trends (Figures S6-S8), albeit based on very few NABA sites (which is why we have shown those results but did not use them in the calculation of the B group risk index). In general we hope that the data organized here for the B group species is an inspiration for greater monitoring of these

taxa with small ranges in regions vulnerable to threats that include ongoing climate change and the loss of natural disturbance regimes (Haddad 2018).

Even greater uncertainty underlies the prioritization of subspecies for conservation, which we have done using a composite of rankings published elsewhere (NatureServe) and a survey of the last year of a publicly reported observation. Despite the uncertainty and different approaches involved in ranking species and subspecies, it is noteworthy that the subspecific risk values are correlated ($r = 0.28$) with risk values for the associated B group species. Not surprisingly given their well-known propensity for subspecific differentiation and localized population dynamics, 44% of the top 50 subspecies (Table 1) are in the family Lycaenidae. Our ranking of subspecies also highlights two states with high numbers of at risk subspecies. First, 25 of the top 50 taxa have a range that includes California, reflecting the long-standing risks to butterfly populations and endemic subspecies from various types of habitat loss and degradation in that state (Forister et al. 2016). Second, 21 of the top 50 taxa have a range that includes Nevada, a region of high subspecific diversity and endemism for many butterfly species across families. In particular, the extreme subspecific diversity of *Euphilotes* species in the western US is apparent and should be a target for future investigation with resurveys, conservation genetics and targeted monitoring; more than 50 *Euphilotes* subspecies are listed in Pelham (2022).

Finally, we can also note that several subspecies in our top list are either protected federally or currently in review for protection under the US Endangered Species Act, but those are intermixed with many taxa in the top 50, and especially the top 25, not receiving federal conservation attention. In addition, while some state agencies in the west manage proactive conservation efforts that prevent species from needing federal protection (e.g., through a list of Species of Greatest Conservation Need [FWS 2001]), other state wildlife agencies do not have

regulatory authority over terrestrial invertebrates. Perhaps our most important finding for subspecies is not reflected in Table 1: of the more than 1k taxa that we reviewed, approximately 400 are not included in NatureServe assessments. Thus the need for broader evaluation is great, and is also urgent as there are many examples of subspecies that have not been seen in many years; these include *Philotiella speciosa bohartorum* with no sightings since the 1970s despite extensive searches (Davenport 2007), *Plebejus* [*Icaricia*] *saepiolus aureolus* presumed extinct from development, and *Euchloe ausonides andrewsi*, threatened by fires and drought and with its last available observation from 1983 (Davenport 2018, SCAN 2022).

CAVEATS & CONCLUSIONS

Our synthesis of status and trends for a diverse fauna faced many challenges. Chief among these is the fact that even for species that are relatively well represented in monitoring schemes, the information is still clustered around areas of human population density. Thus, broad ranges (e.g., Figure 4) and more narrow ranges (e.g., Figure 6) alike are not particularly well sampled in terms of spread of monitored locations in space. We can hope that coming years will see greater investment in monitoring and participation by the general public, and we hope that our use of iNaturalist data in particular encourages both increasing contributions by the general public and the development of new models that can take advantage of mixed data types (e.g, Strebel et al. 2022). Another major data issue that we faced was at the US-Mexico border; although ranges are more recently available for species in Mexico (Glassberg 2018), we have limited our studies for now to north of the border (and south of the Canadian border). We did this partly because of our previous focus on butterflies of the 11 western US states (Forister et al. 2021), but also because one has to bite off a manageable problem which in this case involved stopping at political

borders. We note, however, that the political border especially in the south created many apparently small ranges for those species just crossing that line. Most seriously, those very small ranges are subject to stochasticity in our assessment of exposure to development because a pixel of development can by chance be included or not in small ranges and thus have an outsized influence (in terms of the fraction of the range exposed to development). Better integration of data across southern and northern US borders is an important area for future work, especially since threats involving development or pesticide use could be different in different countries. In the meantime, it is for these reasons that we have included our qualitative range labels (N, S, E, and W) with our rankings (Figure 3). For the B group species in particular, those labels can be used to focus on western species where the political boundaries are considerably less of an issue.

The traditional focus for butterfly conservation in the United States has been at the taxonomic level of subspecies, which is partly a consequence of the fact that population segments cannot be listed for invertebrates (thus leaving subspecies as the next unit below full species that can be protected). We have organized subspecific information and present a list of subspecies that could be profitable targets of conservation attention (Table 1), though most of our effort has been at the level of full species. Thus, we acknowledge that our results fall partly outside of the traditional scope of conservation work for butterflies in the United States. It is, however, entirely likely that compounding population losses across the wild spaces of the region have pushed many full species to the point where range-wide research and conservation attention are warranted. A notable example of this is recent effort focused on conservation of the monarch butterfly, *Danaus plexippus* (Pelton et al. 2019), which is indeed in our list of the 50 most at-risk species (Figure 3), but a number of species are higher on the list and are equally deserving of attention. It is our chief hope that the work presented here is a framework that will facilitate

933 such work in coming decades, acknowledging the many assumptions that have been made along
934 the way.
935

936 **ACKNOWLEDGEMENTS**

937 MLF thanks the National Science Foundation (DEB-2114793), and CAH was supported by a
938 National Institute of Food and Agriculture fellowship (NEVW-2021-09427). EMG, KLB, and
939 JPJ were supported by the Modelscape Consortium with funding from NSF (OIA-2019528).
940 Thanks to the Plant Insect Group at UNR for much thoughtful feedback, and Lee Dyer in
941 particular for various key ideas, as well as Sarina Jepsen who provided important feedback on
942 subspecies risk. We thank Texas State University for the use of the LEAP computing cluster,
943 and thanks also to authors of our previous analysis of western butterflies (Forister et al. 2021)
944 without which the current paper would not have gotten off the ground.
945

946 **CONFLICT OF INTEREST**

947 The authors declare no conflict of interest.
948

949 **AUTHOR CONTRIBUTIONS**

950 MLF conceived the project and the overall organization of data and the presentation of results.
951 TVR wrote the Bayesian population models for the NABA data and contributed to the design of
952 analyses. EMG contributed to numerous components, especially the analysis of spatial data. KJB
953 organized information on subspecies. CAH, CFC, KLB, and TB contributed to component
954 analyses and assisted with data collation or organization. JZ, QC, and NVG generated the
955 phylogeny which was analyzed here by JPJ. JG manages the collection of NABA data and

956 contributed the expert-derived range outlines. AMS has collected the vast majority of the Shapiro
957 transect data (with a few recent years of collection contributed in part by MLF and CAH). All
958 authors contributed to interpretation of results and writing of the manuscript.
959

960 **DATA AVAILABILITY STATEMENT**

961 Data and code will be made available through Dryad at the time the manuscript is accepted for
962 publication.
963

964 **REFERENCES**

965 Abatzoglou, J. T., S. Z. Dobrowski, and S. A. Parks. 2020. Multivariate climate departures have
966 outpaced univariate changes across global lands. Scientific Reports 10:1–9.
967 Abatzoglou, J. T., S. Z. Dobrowski, S. A. Parks, and K. C. Hegewisch. 2018. TerraClimate, a
968 high-resolution global dataset of monthly climate and climatic water balance from 1958–
969 2015. Scientific Data 5:170191.
970 Altschul, S. F., T. L. Madden, A. A. Schäffer, J. Zhang, Z. Zhang, W. Miller, and D. J. Lipman.
971 1997. Gapped BLAST and PSI-BLAST: a new generation of protein database search
972 programs. Nucleic acids research 25:3389–3402.
973 Benton, T. G. 2003. Understanding the ecology of extinction: are we close to the critical
974 threshold? Annales Zoologici Fennici 40:71–80.
975 Bonelli, S., L. P. Casacci, F. Barbero, C. Cerrato, L. Dapporto, V. Sbordoni, S. Scalercio, A.
976 Zilli, A. Battistoni, and C. Teofili. 2018. The first red list of Italian butterflies. Insect
977 Conservation and Diversity 11:506–521.
978 Brook, B. W., N. S. Sodhi, and C. J. A. Bradshaw. 2008. Synergies among extinction drivers

979 under global change. Trends in Ecology & Evolution 23:453–460.

980 Cardoso, P., P. S. Barton, K. Birkhofer, F. Chichorro, C. Deacon, T. Fartmann, C. S. Fukushima,
981 R. Gaigher, J. C. Habel, and C. A. Hallmann. 2020. Scientists' warning to humanity on
982 insect extinctions. Biological Conservation 242:108426.

983 Cardoso, P., T. L. Erwin, P. A. V Borges, and T. R. New. 2011. The seven impediments in
984 invertebrate conservation and how to overcome them. Biological Conservation 144:2647–
985 2655.

986 Casner, K., M. L. Forister, K. Ram, and A. M. Shapiro. 2014a. The utility of repeated presence-
987 absence data as a surrogate for counts: a case study using butterflies. Ecological
988 Applications 18:13–27.

989 Casner, K. L., M. L. Forister, J. M. O'Brien, J. H. Thorne, D. P. Waetjen, and A. M. Shapiro.
990 2014b. Loss of agricultural land and a changing climate contribute to decline of an urban
991 butterfly fauna. Conservation Biology 28:773–782.

992 Crossley, M. S., A. R. Meier, E. M. Baldwin, L. L. Berry, L. C. Crenshaw, G. L. Hartman, D.
993 Lagos-Kutz, D. H. Nichols, K. Patel, and S. Varriano. 2020. No net insect abundance and
994 diversity declines across US Long Term Ecological Research sites. Nature Ecology &
995 Evolution 4:1368–1367.

996 Crossley, M. S., O. M. Smith, L. L. Berry, R. Phillips-Cosio, J. Glassberg, K. M. Holman, J. G.
997 Holmquest, A. R. Meier, S. A. Varriano, and M. R. McClung. 2021. Recent climate change
998 is creating hotspots of butterfly increase and decline across North America. Global Change
999 Biology 27:2702–2714.

1000 Davenport, K. 2007. Yosemite Butterflies. The Taxonomic Report 5.

1001 Davenport, K. 2018. Butterflies of southern California in 2018: updating Emmel and Emmel's

1973 Butterflies of southern California. Lepidoptera of North America 15. Contributions of the CP Gillette Museum of Arthropod Diversity, Colorado State University. Fort Collins, CO.

Diniz-Filho, J. A. F., P. De Marco Jr, and B. A. Hawkins. 2010. Defying the curse of ignorance: perspectives in insect macroecology and conservation biogeography. Insect Conservation and Diversity 3:172–179.

Dirzo, R., H. S. Young, M. Galetti, G. Ceballos, N. J. B. Isaac, and B. Collen. 2014. Defaunation in the Anthropocene. Science 345:401–406.

Edge, D. A., and S. Mecenero. 2015. Butterfly conservation in southern Africa. Journal of Insect Conservation 19:325–339.

Eisenhauer, N., A. Bonn, and C. A Guerra. 2019. Recognizing the quiet extinction of invertebrates. Nature Communications 10:1–3.

Eskildsen, A., L. G. Carvalheiro, W. D. Kissling, J. C. Biesmeijer, O. Schweiger, and T. T. Høye. 2015. Ecological specialization matters: long-term trends in butterfly species richness and assemblage composition depend on multiple functional traits. Diversity and Distributions 21:792–802.

Evans, J. S., and K. Ram. 2021. Package 'spatialEco.' R CRAN Project.

Faber-Langendoen, D., J. Nichols, L. Master, K. Snow, A. Tomaino, R. Bittman, G. Hammerson, B. Heidel, L. Ramsay, and A. Teucher. 2012. NatureServe conservation status assessments: methodology for assigning ranks, https://www.natureserve.org/sites/ default/files/ natureserveconservationstatusmethodology_jun12.pdf. NatureServe, Arlington, VA.

Farber, O., and R. Kadmon. 2003. Assessment of alternative approaches for bioclimatic modeling with special emphasis on the Mahalanobis distance. Ecological Modelling

1025 160:115–130.

1026 Forister, M. L., B. Cousens, J. G. Harrison, K. Anderson, J. H. Thorne, D. Waetjen, C. C. Nice,
1027 M. De Parsia, M. L. Hladik, and R. Meese. 2016. Increasing neonicotinoid use and the
1028 declining butterfly fauna of lowland California. Biology Letters 12:20160475.

1029 Forister, M. L., J. A. Fordyce, C. C. Nice, J. H. Thorne, D. P. Waetjen, and A. M. Shapiro. 2018.
1030 Impacts of a millennium drought on butterfly faunal dynamics. Climate Change Responses
1031 5:3.

1032 Forister, M. L., C. A. Halsch, C. C. Nice, J. A. Fordyce, T. E. Dilts, J. C. Oliver, K. L. Prudic, A.
1033 M. Shapiro, J. K. Wilson, and J. Glassberg. 2021. Fewer butterflies seen by community
1034 scientists across the warming and drying landscapes of the American West. Science
1035 371:1042–1045.

1036 Forister, M. L., A. C. McCall, N. J. Sanders, J. A. Fordyce, J. H. Thorne, J. O'Brien, D. P.
1037 Waetjen, and A. M. Shapiro. 2010. Compounded effects of climate change and habitat
1038 alteration shift patterns of butterfly diversity. Proceedings of the National Academy of
1039 Sciences of the United States of America 107:2088–2092.

1040 Forister, M. L., and A. M. Shapiro. 2003. Climatic trends and advancing spring flight of
1041 butterflies in lowland California. Global Change Biology 9:1130–1135.

1042 Fox, R. 2013. The decline of moths in Great Britain: a review of possible causes. Insect
1043 Conservation and Diversity 6:5–19.

1044 Fox, R., M. S. Warren, T. M. Brereton, D. B. Roy, and A. Robinson. 2011. A new Red List of
1045 British butterflies. Insect Conservation and Diversity 4:159–172.

1046 FWS. 2001. Fish and Wildlife Service, Department of the Interior. 2001. 50 Million FY 2001
1047 Wildlife Conservation and Restoration Account, 50 Million FY 2001 State Wildlife Grants

1048 Program. Federal Register 66:7657–7660.
1049 GBIF.org. 2021a. GBIF Occurrence Download (Papilionidae)
1050 https://doi.org/10.15468/dl.m652hd.
1051 GBIF.org. 2021b. GBIF Occurrence Download (Hesperiidae) https://doi.org/10.15468/dl.dcthdd.
1052 GBIF.org. 2021c. GBIF Occurrence Download (Nymphalidae)
1053 https://doi.org/10.15468/dl.qzgtcr.
1054 GBIF.org. 2021d. GBIF Occurrence Download (Lycaenidae) https://doi.org/10.15468/dl.2j2ay4.
1055 GBIF.org. 2021e. GBIF Occurrence Download (Pieridae) https://doi.org/10.15468/dl.vquqtz.
1056 GBIF.org. 2021f. GBIF Occurrence Download (Riodinidae) https://doi.org/10.15468/dl.bbtkq2.
1057 Geyle, H. M., M. F. Braby, M. Andren, E. P. Beaver, P. Bell, C. Byrne, M. Castles, F. Douglas,
1058 R. V Glatz, and B. Haywood. 2021. Butterflies on the brink: identifying the Australian
1059 butterflies (Lepidoptera) most at risk of extinction. Austral Entomology 60:98–110.
1060 Glassberg, J. 2017. A Swift guide to butterflies of North America. Princeton University Press.
1061 Glassberg, J. 2018. A Swift guide to butterflies of Mexico and Central America. Princeton
1062 University Press.
1063 Gonzalez, P., F. Wang, M. Notaro, D. J. Vimont, and J. W. Williams. 2018. Disproportionate
1064 magnitude of climate change in United States national parks. Environmental Research
1065 Letters 13:104001.
1066 Goulson, D. 2019. The insect apocalypse, and why it matters. Current Biology 29:R967–R971.
1067 Haddad, N. M. 2018. Resurrection and resilience of the rarest butterflies. PLoS Biology
1068 16:e2003488.
1069 Hallmann, C. A., M. Sorg, E. Jongejans, H. Siepel, N. Hofland, H. Schwan, W. Stenmans, A.
1070 Müller, H. Sumser, T. Hörren, and others. 2017. More than 75 percent decline over 27 years

1071 in total flying insect biomass in protected areas. PlOS ONE 12:e0185809.
1072 Halsch, C. A., A. M. Shapiro, J. A. Fordyce, C. C. Nice, J. H. Thorne, D. P. Waetjen, and M. L.
1073 Forister. 2021. Insects and recent climate change. Proceedings of the National Academy of
1074 Sciences:10.1073/pnas.2002543117.
1075 Hamilton, H., R. L. Smyth, B. E. Young, T. G. Howard, C. Tracey, S. Breyer, D. R. Cameron, A.
1076 Chazal, A. K. Conley, and C. Frye. 2022. Increasing taxonomic diversity and spatial
1077 resolution clarifies opportunities for protecting imperiled species in the US. Ecological
1078 Applications:e2534.
1079 Hawkins, B. A. 2010. Multiregional comparison of the ecological and phylogenetic structure of
1080 butterfly species richness gradients. Journal of Biogeography 37:647–656.
1081 Hijmans, R. J., J. van Etten, M. Mattiuzzi, M. Sumner, J. A. Greenberg, O. P. Lamingueiro, A.
1082 Bevan, E. B. Racine, and A. Shortridge. 2021. raster: Geographic Data Analysis and
1083 Modeling, Version 2.9-23, R package.
1084 Hochmair, H. H., R. H. Scheffrahn, M. Basille, and M. Boone. 2020. Evaluating the data quality
1085 of iNaturalist termite records. PLOS ONE 15:e0226534.
1086 Hughes, J. B., G. C. Daily, and P. R. Ehrlich. 2000. Conservation of insect diversity: a habitat
1087 approach. Conservation Biology 14:1788–1797.
1088 Jamwal, P. S., M. Di Febbraro, M. L. Carranza, M. Savage, and A. Loy. 2021. Global change on
1089 the roof of the world: Vulnerability of Himalayan otter species to land use and climate
1090 alterations. Diversity and Distributions.
1091 Janzen, D. H., and W. Hallwachs. 2019. Perspective: Where might be many tropical insects?
1092 Biological Conservation 233:102–108.
1093 Katoh, K., K. Misawa, K. Kuma, and T. Miyata. 2002. MAFFT: a novel method for rapid

1094 multiple sequence alignment based on fast Fourier transform. Nucleic Acids Research
1095 30:3059–3066.
1096 Kellner, K. 2017. R Package 'jagsUI': a wrapper around 'rjags' to streamline 'JAGS'Analyses,
1097 v.1.4.9.
1098 Kirchhoff, C., C. T. Callaghan, D. A. Keith, D. Indiarto, G. Taseski, M. K. J. Ooi, T. D. Le
1099 Breton, T. Mesaglio, R. T. Kingsford, and W. K. Cornwell. 2021. Rapidly mapping fire
1100 effects on biodiversity at a large-scale using citizen science. Science of The Total
1101 Environment 755:142348.
1102 van Klink, R., D. E. Bowler, K. B. Gongalsky, A. B. Swengel, A. Gentile, and J. M. Chase.
1103 2020. Meta-analysis reveals declines in terrestrial but increases in freshwater insect
1104 abundances. Science 368:417–420.
1105 Li, L., C. J. Stoeckert, and D. S. Roos. 2003. OrthoMCL: identification of ortholog groups for
1106 eukaryotic genomes. Genome Research 13:2178–2189.
1107 Maes, D., W. Vanreusel, I. Jacobs, K. Berwaerts, and H. Van Dyck. 2012. Applying IUCN Red
1108 List criteria at a small regional level: a test case with butterflies in Flanders (north
1109 Belgium). Biological Conservation 145:258–266.
1110 McLaughlin, J. F., J. J. Hellmann, C. L. Boggs, and P. R. Ehrlich. 2002. Climate change hastens
1111 population extinctions. Proceedings of the National Academy of Sciences of the United
1112 States of America 99:6070–6074.
1113 NABA. 2018. Checklist of North American Butterflies Occurring North of Mexico - Edition 2.4.
1114 Naeem, S., R. Chazdon, J. E. Duffy, C. Prager, and B. Worm. 2016. Biodiversity and human
1115 well-being: an essential link for sustainable development. Proceedings of the Royal Society
1116 B: Biological Sciences 283:20162091.

1117 Nakamura, Y. 2011. Conservation of butterflies in Japan: status, actions and strategy. Journal of
1118 Insect Conservation 15:5–22.
1119 New, T. R., R. M. Pyle, J. A. Thomas, C. D. Thomas, and P. C. Hammond. 1995. Butterfly
1120 Conservation Management. Annual Review of Entomology 40:57–83.
1121 Nguyen, L.-T., H. A. Schmidt, A. Von Haeseler, and B. Q. Minh. 2015. IQ-TREE: a fast and
1122 effective stochastic algorithm for estimating maximum-likelihood phylogenies. Molecular
1123 Biology and Evolution 32:268–274.
1124 Nice, C. C., M. L. Forister, Z. Gompert, J. A. Fordyce, and A. M. Shapiro. 2014. A hierarchical
1125 perspective on the diversity of butterfly species' responses to weather in the Sierra Nevada
1126 Mountains. Ecology 95:2155–2168.
1127 Opler, P. A. 1999. A field guide to western butterflies. Houghton Mifflin Harcourt.
1128 Pelham, J. P. 2022. A catalogue of the butterflies of the United States and Canada.
1129 Pelton, E. M., C. B. Schultz, S. J. Jepsen, S. H. Black, and E. E. Crone. 2019. Western monarch
1130 population plummets: status, probable causes, and recommended conservation actions.
1131 Frontiers in Ecology and Evolution 7:258.
1132 Pilliod, D. S., M. I. Jeffries, R. S. Arkle, and D. H. Olson. 2020. Reptiles under the conservation
1133 umbrella of the greater sage-grouse. The Journal of Wildlife Management 84:478–491.
1134 Prudic, K. L., J. C. Oliver, B. V Brown, and E. C. Long. 2018. Comparisons of citizen science
1135 data-gathering approaches to evaluate urban butterfly diversity. Insects 9:186.
1136 RCoreTeam. 2020. R: A language and environment for statistical computing R Foundation for
1137 Statistical Computing, Vienna, Austria. URL https://www.R-project.org/.
1138 Revell, L. J. 2012. phytools: an R package for phylogenetic comparative biology (and other
1139 things). Methods in Ecology and Evolution:217–223.

1140 Riecke, T. V, D. Gibson, M. Kéry, and M. Schaub. 2021. Sharing detection heterogeneity
1141 information among species in community models of occupancy and abundance can
1142 strengthen inference. Ecology and evolution 11:18125–18135.
1143 Salcido, D. M., M. L. Forister, H. G. Lopez, and L. A. Dyer. 2020. Ecosystem services at risk
1144 from declining taxonomic and interaction diversity in a tropical forest. Scientific Reports
1145 10:1–10.
1146 Samways, M. J. 2007. Insect conservation: a synthetic management approach. Annu. Rev.
1147 Entomol. 52:465–487.
1148 SCAN. 2022. Symbiota Collections of Arthropods Network https://scan-bugs.org/portal/.
1149 Schultz, C. B., N. M. Haddad, E. H. Henry, and E. E. Crone. 2019. Movement and demography
1150 of at-risk butterflies: building blocks for conservation. Annual Review of Entomology
1151 64:167–184.
1152 Scott, J. A. 1986. The butterflies of North America. Stanford University Press, Stanford,
1153 California.
1154 Sekar, S. 2012. A meta-analysis of the traits affecting dispersal ability in butterflies: can
1155 wingspan be used as a proxy? Journal of Animal Ecology 81:174–184.
1156 Sen, P. K. 1968. Estimates of the regression coefficient based on Kendall's tau. Journal of the
1157 American Statistical Association 63:1379–1389.
1158 Shapiro, A. M. 1996. Status of butterflies. Pages 743–757 Sierra Nevada Ecosystem Project:
1159 Final Report to Congress Vol. II. Center for Water and Wildland Resources, University of
1160 California, Davis, Davis, California.
1161 Shapiro, A. M. 2022. Art Shapiro's Butterfly Site https://butterfly.ucdavis.edu/.
1162 Staude, I. R., L. M. Navarro, and H. M. Pereira. 2020. Range size predicts the risk of local

extinction from habitat loss. Global Ecology and Biogeography 29:16–25.

Strebel, N., M. Kéry, J. Guélat, and T. Sattler. 2022. Spatiotemporal modelling of abundance from multiple data sources in an integrated spatial distribution model. Journal of Biogeography 49:563–575.

van Swaay, C., D. Maes, S. Collins, M. L. Munguira, M. Šašić, J. Settele, R. Verovnik, M. Warren, M. Wiemers, and I. Wynhoff. 2011. Applying IUCN criteria to invertebrates: How red is the Red List of European butterflies? Biological Conservation 144:470–478.

Theil, H. 1950. A rank-invariant method of linear and polynomial regression analysis. Indagationes Mathematicae 12:173.

Turvey, S. T., and J. J. Crees. 2019. Extinction in the Anthropocene. Current Biology 29:R982–R986.

USDA. 2020. National Agricultural Statistics Service Cropland Data Layer. Published crop-specific data layer. https://nassgeodata.gmu.edu/CropScape/.

Wagner, D. L. 2019. Insect declines in the Anthropocene. Annual Review of Entomology 65.

Wepprich, T., J. R. Adrion, L. Ries, J. Wiedmann, and N. M. Haddad. 2019. Butterfly abundance declines over 20 years of systematic monitoring in Ohio, USA. PLOS ONE 14:e0216270.

Wilson, E. O. 1987. The little things that run the world (the importance and conservation of invertebrates). Conservation Biology 1:344–346.

Wilson, J. S., A. D. Pan, D. E. M. General, and J. B. Koch. 2020. More eyes on the prize: an observation of a very rare, threatened species of Philippine Bumble bee, *Bombus irisanensis*, on iNaturalist and the importance of citizen science in conservation biology. Journal of Insect Conservation 24:727–729.

Yu, G., D. K. Smith, H. Zhu, Y. Guan, and T. T. Lam. 2017. ggtree: an R package for

1186 visualization and annotation of phylogenetic trees with their covariates and other associated
1187 data. Methods in Ecology and Evolution 8:28–36.
1188 Zhang, J., Q. Cong, J. Shen, P. A. Opler, and N. V Grishin. 2019. Genomics of a complete
1189 butterfly continent. BioRxiv:829887.

1190

1191

TABLE 1. Top 50 subspecies ranked by quantitative risk index, including taxonomic name and family, states in which subspecies are found, as well as the species group (A or B) to which the nominal species belongs. The taxonomy used here is based on Pelham (2022) because of the emphasis on subspecific distinctions; where the generic or specific names differ from NABA (2018), the alternative name is in brackets (exceptions to that are the *Euphilotes* taxa, for which taxonomy and differences in usage are complex; in those cases we have not listed synonymies between Pelham and NABA); common names are also given here as they are more stable for some subspecies than trinomials. Species marked with an asterisk (*) are protected by the US Endangered Species Act; ** = currently under review for protection.

Risk	Subspecies	States	Family	Group
0.837	*Philotiella speciosa bohartorum*, Bohart's small blue	CA	Lycaenidae	B
0.750	*Argynnis* [*Speyeria*] *adiaste adiaste*, unsilvered fritillary	CA	Nymphalidae	B
0.723	*Euchloe hyantis andrewsi*, Andrew's marble	CA	Pieridae	A
0.720	*Icaricia* [*Plebejus*] *saepiolus aureolus*, San Gabriel Mtns greenish blue	CA	Lycaenidae	A
0.712	*Euphilotes pallescens mattonii*, Mattoni's blue	NV	Lycaenidae	B
0.692	*Cercyonis oetus alkalorum*, small wood-nymph	NV	Nymphalidae	A
0.677	*Argynnis* [*Speyeria*] *nokomis nokomis*, Great Basin nokomis fritillary **	AZ, CO, NM, UT	Nymphalidae	B
0.677	*Euphilotes pallescens arenamontana*, San Mountain blue	NV	Lycaenidae	B
0.677	*Euphilotes pallescens calneva*, Honey Lake blue	CA, NV	Lycaenidae	B
0.677	*Hesperia miriamae longaevicola*, White Mountains skipper	CA, NV	Hesperiidae	B
0.677	*Satyrium polingi organensis*, Organ Mountains Poling's hairstreak	NM	Lycaenidae	B
0.677	*Euphilotes pallescens ricei*, Rice's blue	NV	Lycaenidae	B
0.677	*Philotiella speciosa septentrionalis*, Great Basin small blue	NV	Lycaenidae	B
0.664	*Euphilotes enoptes primavera*, dotted blue	NV	Lycaenidae	A
0.654	*Megathymus ursus deserti*, desert yucca borer	AZ	Hesperiidae	B
0.653	*Argynnis* [*Speyeria*] *nokomis carsonensis*, Carson Valley nokomis fritillary	CA, NV	Nymphalidae	B
0.650	*Colias skinneri* [*pelidne*] *hinchliffi*, Skinner's pelidne sulphur	OR	Pieridae	B
0.629	*Callophrys mossii bayensis*, San Bruno elfin *	CA	Lycaenidae	A
0.629	*Callophrys mossii marinensis*, Moss' elfin *	CA	Lycaenidae	A
0.629	*Euphilotes bernardino minuta*, Baking Powder Flat blue	NV	Lycaenidae	A
0.629	*Hesperia leonardus montana*, Leonard's skipper *	CO	Hesperiidae	B
0.629	*Euphilotes mojave virginensis*, Virgin Mountains Mojave blue	AZ, NV, UT	Lycaenidae	A
0.626	*Hesperia uncas fulvapalla*, Uncas skipper	NV	Hesperiidae	B
0.609	*Argynnis* [*Speyeria*] *egleis yolaboli*, Great Basin fritillary	CA	Nymphalidae	A
0.605	*Pseudocopaeodes eunus alinea*, Eunus skipper	CA, NV	Hesperiidae	B
0.605	*Hesperia uncas giulianii*, Railroad Valley skipper	CA	Hesperiidae	B
0.605	*Hesperia uncas grandiosa*, Big Smoky Valley skipper	NV	Hesperiidae	B
0.605	*Callophrys loki* [*gryneus*] *thornei*, Thorne's hairstreak	CA	Lycaenidae	A
0.600	*Cercyonis pegala carsonensis*, Carson Valley wood nymph	CA, NV	Nymphalidae	A
0.591	*Euphilotes battoides fusimaculata*, square dotted blue	NV	Lycaenidae	A
0.581	*Boloria improba acrocnema*, Uncompahgre fritillary *	CO	Nymphalidae	B
0.581	*Phyciodes cocyta* [selenis] *arenacolor*, Steptoe Valley crescent	NV	Nymphalidae	A
0.581	*Euphilotes enoptes aridorum*, dotted blue	CA, NV	Lycaenidae	A
0.581	*Argynnis* [*Speyeria*] *zerene behrensii*, Behren's silverspot *	CA	Nymphalidae	A
0.581	*Argynnis* [*Speyeria*] *callippe callippe*, Callippe silverspot *	CA	Nymphalidae	A
0.581	*Icaricia* [*Plebejus*] *shasta charlestonensis*, Mt. Charleston blue *	CA	Lycaenidae	A
0.581	*Euphydryas anicia* [*chalcedona*] *cloudcrofti*, Sacramento Mtns checkerspot	NM	Nymphalidae	A
0.581	*Euphilotes pallescens emmeli*, Emmel's blue	AZ, NV, UT	Lycaenidae	A
0.581	*Icaricia* [*Plebejus*] *icarioides fenderi*, Fender's blue *	OR	Lycaenidae	A
0.581	*Argynnis* [*Speyeria*] *zerene hippolyta*, Oregon silverspot *	CA, OR, WA	Nymphalidae	A
0.581	*Euchloe ausonides insulanus*, island marble *	WA	Pieridae	A
0.581	*Pyrgus ruralis lagunae*, Laguna Mountains skipper *	CA	Hesperiidae	A
0.581	*Apodemia mormo langei*, Lange's metalmark *	CA	Riodinidae	A
0.581	*Icaricia* [*Plebejus*] *icarioides missionensis*, Mission blue *	CA	Lycaenidae	A
0.581	*Ceryconis oetus pallescens*, small wood-nymph	NV	Nymphalidae	A
0.581	*Glaucopsyche lygdamus palosverdesensis*, Palos Verde blue *	CA	Lycaenidae	A
0.581	*Polites sabuleti sinemaculata*, bleached sandhill skipper	NV	Hesperiidae	A
0.581	*Argynnis* [*Speyeria*] *zerene sonomensis*, Zerene fritillary	CA	Nymphalidae	A
0.581	*Euphydryas editha taylori*, Taylor's checkerspot *	OR, WA	Nymphalidae	A
0.568	*Glaucopsyche piasus gabrielina*, San Gabriel Mtns arrowhead blue	CA	Lycaenidae	A

1192

1193 **Figure legends**

1194

1195 **FIGURE 1** Schematic overview of main inputs, processes and products associated with the
1196 generation of risk index values for species (subspecies are treated separately). As noted in the
1197 key, data sources are in brown, analyses (and other calculations) are in blue boxes, variables
1198 (used in the creation of the risk index) are in red, and the primary products are in green. The
1199 central branching path illustrates the division of species into the A and B groups, with
1200 observational data contributing to the A group risk assessment on the left, and other data types
1201 contributing to B group assessment on the right. The 10 variables (in red) are identical to the
1202 columns in Figure 3, although labelled slightly different here, especially for the observational
1203 variables: "β year" is the year coefficient from analyses of Shapiro data summarizing change
1204 through time; "P(persistence)" is the probability of population persistence from 50-year
1205 forecasts, and **Δ** range is an index of change in geographic range based on the relationship
1206 between the last 15 years of iNaturalist observations while controlling for the size of the expert-
1207 derived range. Variables on the right ("range area", "precipitation," etc.) are more self-
1208 explanatory. Also note that the expert-derived geographic ranges contribute to the risk index
1209 calculations both directly ("range area" and "voltinism") and indirectly as indicated with
1210 connecting arrows. Finally, the "Risk analysis" process box (towards the lower left) illustrates
1211 the analysis of A group risk that was used to partly inform the weighting scheme for the B group
1212 species.

1213

1214 **FIGURE 2** Summary of differences between species in the A and B groups. The 184 A group
1215 species are those with observational data from either the Shapiro monitoring program or the

1216 NABA annual counts; the 212 B group species are not included in those data sources (at least not
1217 with sufficient abundance to be used in our primary models). Comparisons in panels (a) through
1218 (g) are shown as violin plots with kernel density estimates and horizontal lines marking medians
1219 inside rectangles spanning interquartile ranges; vertical lines are upper and lower fences
1220 computed as the third quartile plus one and a half times the interquartile range, and the first
1221 quartile minus one and a half times the interquartile range, respectively. Colors in panels (a)
1222 through (f) match those used in Figure 3 for the same variables. Area-weighted latitudinal
1223 midpoints are shown in panel (g), and the mosaic plot in (h) shows the biogeographical
1224 breakdown of qualitative range positions for A and B group species (e.g., species with ranges in
1225 the South category have a majority of their range south of the US-Mexico border, with only a
1226 small presence north of the border in the western US).
1227
1228 **FIGURE 3** The top 50 species with the highest risk rankings in the A group (on the left) and the
1229 B group (on the right). The two panels have some features in common, and some unique
1230 elements. In common they both show the extent to which different variables are associated with
1231 higher or lower risk for each species: a large circle under NABA occupancy, for example, marks
1232 a species that we infer as being at risk because of low forecast occupancy (probability of
1233 population persistence) across currently-extant locations; similarly, a large circle under
1234 development indicates a species at risk because of high exposure to developed lands, and a large
1235 circle under geographic range indicates corresponding risk associated with a relatively small
1236 range. The sizes of the circles were assigned separately within the two lists, A and B group
1237 species, and thus indicate relative differences within those lists. Although all variables are shown
1238 for comparison, the overall risk ranking for the A group species is based solely on the first three

variables (NABA occupancy, Shapiro monitoring, and iNaturalist, to the left of the vertical gray line), while the ranking for the B group species is based entirely on the other seven variables (see main text for details, and Figure 1). Both panels also have in common the quantitative risk values shown to the right (e.g., the risk index for *Vanessa annabella* in panel A is 0.675); note that the risk values for the A group species include 85% credible intervals (in parentheses), encompassing uncertainty derived from Bayesian analyses of both NABA and Shapiro data. The capital letters (N, S, E and W) running down the left side of each panel are qualitative biogeographical descriptions (see main text for details), and the asterisks next to species names flag taxonomic issues (see Table S3). A unique element of the panel on the left is the sample size in parentheses, e.g. "(14,10)" for *Vanessa annabella*, which is the number of locations from which data were included from the NABA and Shapiro datasets, respectively. Finally, on the far right of panel (b), the lambda symbols represent the results of individual time series models run for the species present in the NABA program but without enough sites and years to be included in the main model (and thus not a part of the A list); a blue symbol indicates a species with an 80% or greater probability of increasing in recent years, while a red symbol indicates an 80% chance of decreasing, and black is neither increasing nor decreasing. The other species (beyond the top 50 highest ranked shown here) are included in Figures S6, S7, and S8.

FIGURE 4 Overview of site-specific trends through time for *Vanessa annabella* at Shapiro sites (on the left) and NABA sites (on the right and along the bottom). Plots for Shapiro sites are shown with decreasing elevation (cooler colors are montane sites) and colored to match the elevational profile of Northern California shown below the map of the western US. The y-axes for Shapiro plots are the fraction of days a species was seen at a site in a year (Shapiro data were

truncated at 1984 for analyses, but earlier years are shown here and in Figures 5 and 6). Plots for NABA sites are shown with decreasing latitude (starting with the most northern sites), with symbols matching the locations shown in the central map. Values shown in NABA plots have been adjusted for variation in sampling effort, and values plotted are total counts of individuals on a natural log scale. Finally, the light gray triangles on the central map are locations of iNaturalist records within the last 15 years that were used to estimate the difference between expert-derived geographic range and community scientist-derived area of occupancy (based on the iNaturalist records). Adult and caterpillar images by Camryn Maher, copyright 2022.

FIGURE 5 Overview of site-specific trends through time for *Euchloe ausonides* at Shapiro sites (on the left) and NABA sites (on the right). Plots for Shapiro sites are shown with decreasing elevation (cooler colors are montane sites) and colored to match the elevational profile of Northern California shown below the map of the western US. The y-axes for Shapiro plots are the fraction of days a species was seen at a site in a year. Plots for NABA sites are shown with decreasing latitude (starting with the most northern sites), with symbols matching the locations shown in the central map. Values shown in NABA plots have been adjusted for variation in sampling effort, and values plotted are total counts of individuals on a natural log scale. Finally, the light gray triangles on the central map are locations of iNaturalist records within the last 15 years that were used to estimate the difference between expert-derived geographic range and community scientist-derived area of occupancy (based on the iNaturalist records). Adult and caterpillar images by Camryn Maher, copyright 2022.

FIGURE 6 Overview of site-specific trends through time for *Poanes melane* at Shapiro sites (on the left) and NABA sites (on the right). Plots for Shapiro sites are shown with decreasing elevation (cooler colors are montane sites) and colored to match the elevational profile of Northern California shown below the map of the western US. The y-axes for Shapiro plots are the fraction of days a species was seen at a site in a year. Plots for NABA sites are shown with decreasing latitude (starting with the most northern sites), with symbols matching the locations shown in the central map. Values shown in NABA plots have been adjusted for variation in sampling effort, and values plotted are total counts of individuals on a natural log scale. Finally, the light gray triangles on the central map are locations of iNaturalist records within the last 15 years that were used to estimate the difference between expert-derived geographic range and community scientist-derived area of occupancy (based on the iNaturalist records). Adult and caterpillar images by Camryn Maher, copyright 2022.

FIGURE 7 The geography of risk for species with values in the upper 75th quantile of risk indices as shown in Figure 3 (i.e., combining "medium" and "high" risk categories treated separately in Figure 8). Panels (a) and (b) show average risk values among those high risk species, separately for the A and B group species, while panels (c) and (d) show species richness again for the A group and B group species.

FIGURE 8 The phylogenetic distribution of risk, here shown as three categories: high risk (upper 90th quantile), medium risk (75th to 90th quantiles), and low risk (below the 75th quantile). Species names in black are the A group species, other are B group. Butterfly images as follows: (A) *Apodemia mormo* (Riodinidae); (B) *Euphilotes pallescens arenamontana*

1307 (Lycaenidae); (C) *Euchloe ausonides* (Pieridae); (D) *Polites sabuleti* (Hesperiidae); (E) *Adelpha*
1308 *bredowii* (Nymphalidae); (F) *Papilio rutulus* (Papilionidae). Photo credits go to CAH (panels A,
1309 C, E, and F); MLF (panels B and D). Bootstrap support is not shown but the vast majority of
1310 nodes have support above 0.95; see Zhang et al. (2019) for additional details.

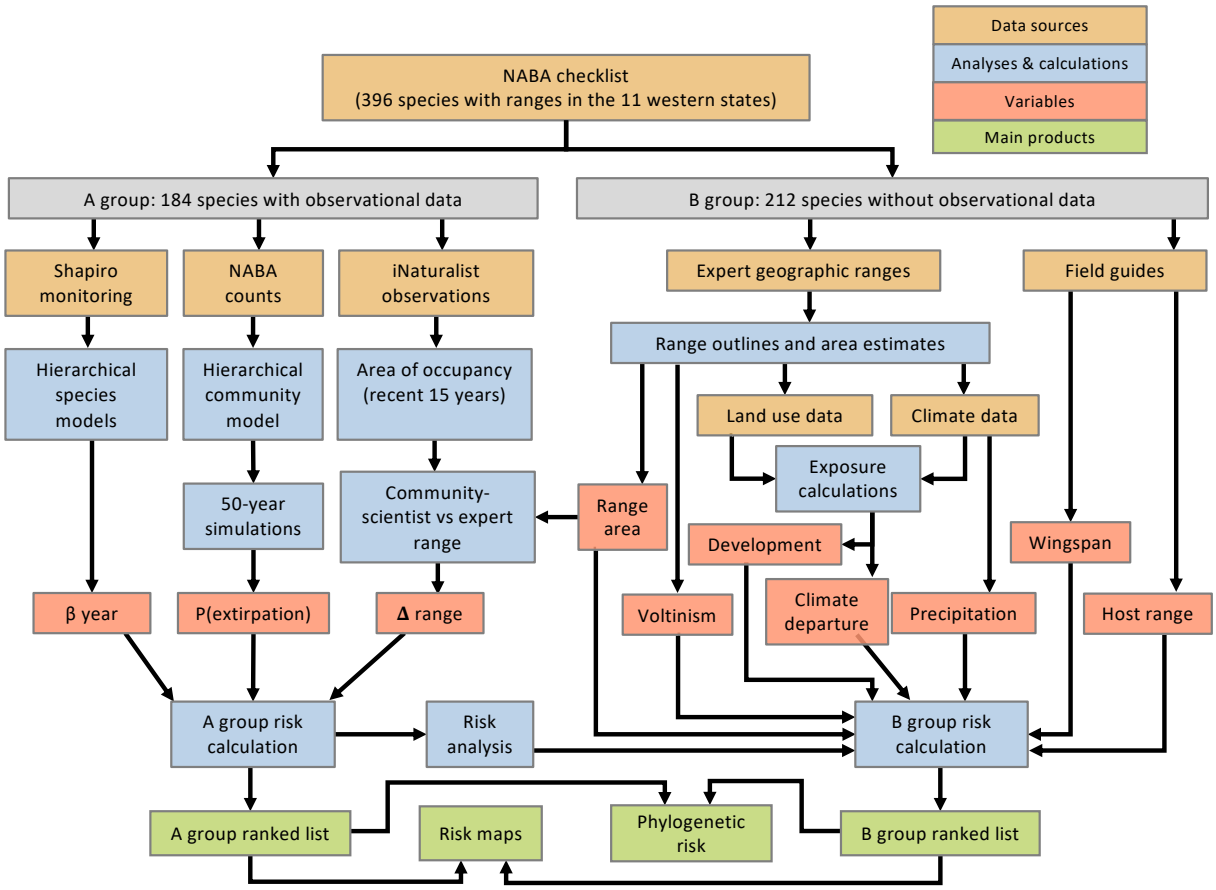
Data sources
Analyses & calculations
Variables
Main products
NABA checklist
(396 species with ranges in the 11 western states)
A group: 184 species with observational data
B group: 212 species without observational data
Shapiro monitoring
NABA counts
iNaturalist observations
Expert geographic ranges
Field guides
Hierarchical species models
Hierarchical community model
Area of occupancy (recent 15 years)
Range outlines and area estimates
Land use data
Climate data
Exposure calculations
50-year simulations
Community-scientist vs expert range
Range area
Development
Wingspan
β year
P(extirpation)
Δ range
Voltinism
Climate departure
Precipitation
Host range
A group risk calculation
Risk analysis
B group risk calculation
A group ranked list
Risk maps
Phylogenetic risk
B group ranked list

Figure 1

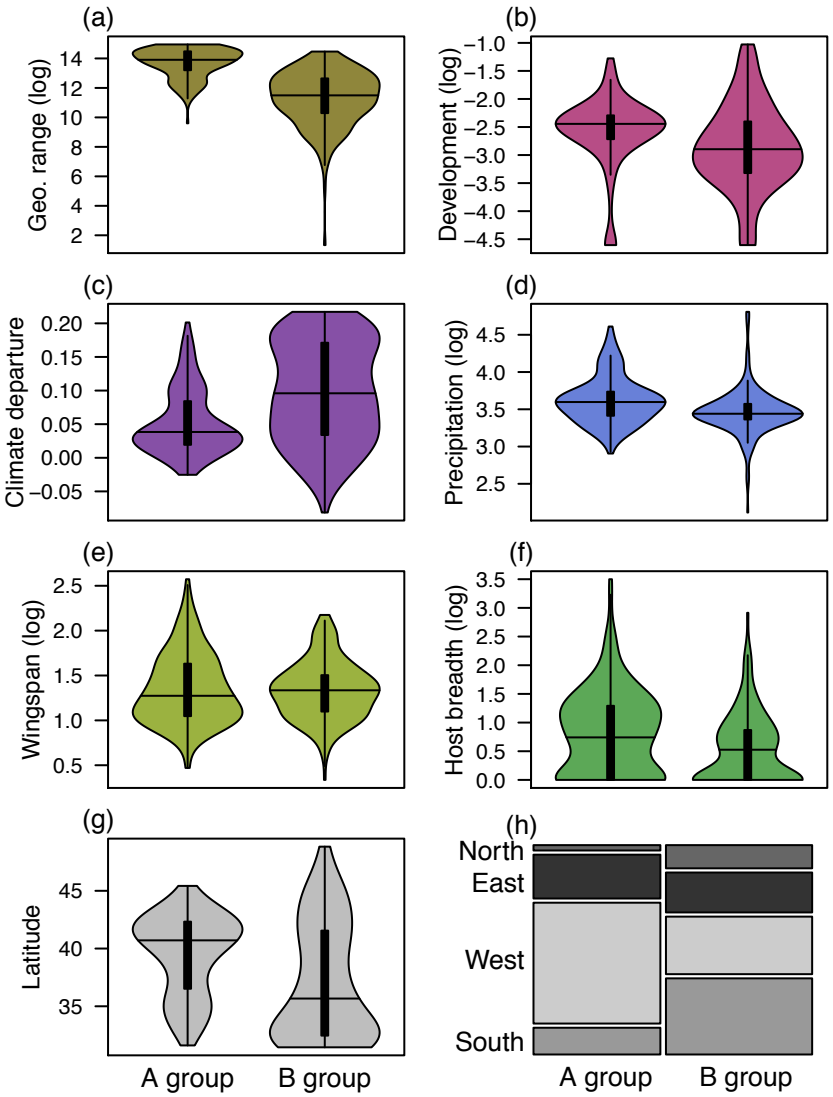
(a)
Geo. range (log)
14
12
10
8
6
4
2
(b)
Development (log)
−1.0
−1.5
−2.0
−2.5
−3.0
−3.5
−4.0
−4.5
(c)
Climate departure
0.20
0.15
0.10
0.05
0.00
−0.05
(d)
Precipitation (log)
4.5
4.0
3.5
3.0
2.5
(e)
Wingspan (log)
2.5
2.0
1.5
1.0
0.5
(f)
Host breadth (log)
3.5
3.0
2.5
2.0
1.5
1.0
0.5
0.0
(g)
Latitude
45
40
35
A group
B group
(h)
North
East
West
South
A group
B group

Figure 2

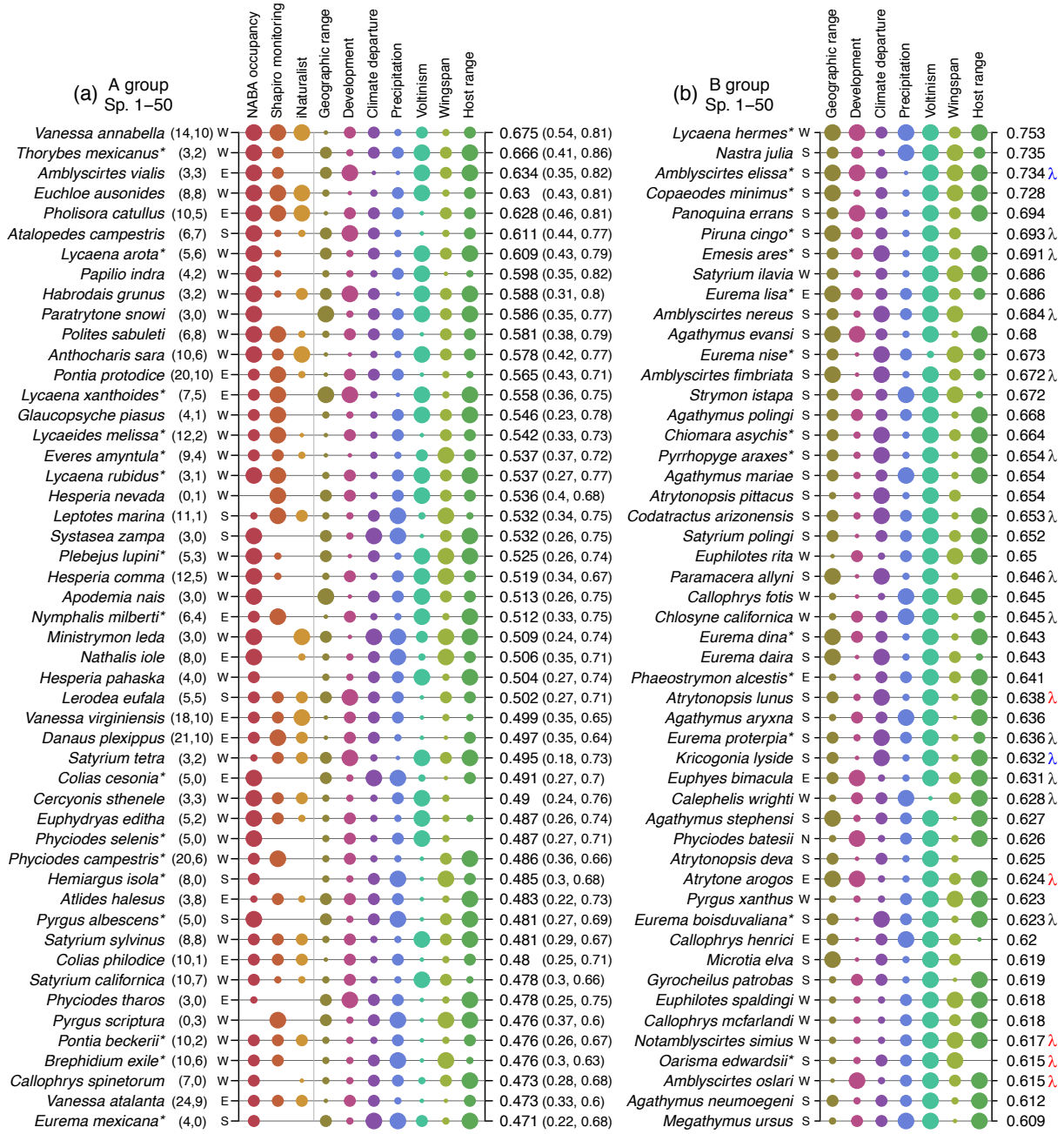
(a) A group Sp. 1–50
NABA occupancy
Shapiro monitoring
iNaturalist
Geographic range
Development
Climate departure
Precipitation
Voltinism
Wingspan
Host range
Vanessa annabella (14,10) W 0.675 (0.54, 0.81)
Thorybes mexicanus* (3,2) W 0.666 (0.41, 0.86)
Amblyscirtes vialis (3,3) E 0.634 (0.35, 0.82)
Euchloe ausonides (8,8) W 0.63 (0.43, 0.81)
Pholisora catullus (10,5) E 0.628 (0.46, 0.81)
Atalopedes campestris (6,7) S 0.611 (0.44, 0.77)
Lycaena arota* (5,6) W 0.609 (0.43, 0.79)
Papilio indra (4,2) W 0.598 (0.35, 0.82)
Habrodais grunus (3,2) W 0.588 (0.31, 0.8)
Paratrytone snowi (3,0) W 0.586 (0.35, 0.77)
Polites sabuleti (6,8) W 0.581 (0.38, 0.79)
Anthocharis sara (10,6) W 0.578 (0.42, 0.77)
Pontia protodice (20,10) E 0.565 (0.43, 0.71)
Lycaena xanthoides* (7,5) E 0.558 (0.36, 0.75)
Glaucopsyche piasus (4,1) W 0.546 (0.23, 0.78)
Lycaeides melissa* (12,2) W 0.542 (0.33, 0.73)
Everes amyntula* (9,4) W 0.537 (0.37, 0.72)
Lycaena rubidus* (3,1) W 0.537 (0.27, 0.77)
Hesperia nevada (0,1) W 0.536 (0.4, 0.68)
Leptotes marina (11,1) S 0.532 (0.34, 0.75)
Systasea zampa (3,0) S 0.532 (0.26, 0.75)
Plebejus lupini* (5,3) W 0.525 (0.26, 0.74)
Hesperia comma (12,5) W 0.519 (0.34, 0.67)
Apodemia nais (3,0) W 0.513 (0.26, 0.75)
Nymphalis milberti* (6,4) E 0.512 (0.33, 0.75)
Ministrymon leda (3,0) W 0.509 (0.24, 0.74)
Nathalis iole (8,0) E 0.506 (0.35, 0.71)
Hesperia pahaska (4,0) W 0.504 (0.27, 0.74)
Lerodea eufala (5,5) S 0.502 (0.27, 0.71)
Vanessa virginiensis (18,10) E 0.499 (0.35, 0.65)
Danaus plexippus (21,10) E 0.497 (0.35, 0.64)
Satyrium tetra (3,2) W 0.495 (0.18, 0.73)
Colias cesonia* (5,0) E 0.491 (0.27, 0.7)
Cercyonis sthenele (3,3) W 0.49 (0.24, 0.76)
Euphydryas editha (5,2) W 0.487 (0.26, 0.74)
Phyciodes selenis* (5,0) W 0.487 (0.27, 0.71)
Phyciodes campestris* (20,6) W 0.486 (0.36, 0.66)
Hemiargus isola* (8,0) S 0.485 (0.3, 0.68)
Atlides halesus (3,8) E 0.483 (0.22, 0.73)
Pyrgus albescens* (5,0) S 0.481 (0.27, 0.69)
Satyrium sylvinus (8,8) W 0.481 (0.29, 0.67)
Colias philodice (10,1) E 0.48 (0.25, 0.71)
Satyrium californica (10,7) W 0.478 (0.3, 0.66)
Phyciodes tharos (3,0) E 0.478 (0.25, 0.75)
Pyrgus scriptura (0,3) W 0.476 (0.37, 0.6)
Pontia beckerii* (10,2) W 0.476 (0.26, 0.67)
Brephidium exile* (10,6) W 0.476 (0.3, 0.63)
Callophrys spinetorum (7,0) W 0.473 (0.28, 0.68)
Vanessa atalanta (24,9) E 0.473 (0.33, 0.6)
Eurema mexicana* (4,0) S 0.471 (0.22, 0.68)
(b) B group Sp. 1–50
Geographic range
Development
Climate departure
Precipitation
Voltinism
Wingspan
Host range
Lycaena hermes* W 0.753
Nastra julia S 0.735
Amblyscirtes elissa* S 0.734 λ
Copaeodes minimus* S 0.728
Panoquina errans S 0.694
Piruna cingo* S 0.693 λ
Emesis ares* S 0.691 λ
Satyrium ilavia W 0.686
Eurema lisa* E 0.686
Amblyscirtes nereus S 0.684 λ
Agathymus evansi S 0.68
Eurema nise* S 0.673
Amblyscirtes fimbriata S 0.672 λ
Strymon istapa S 0.672
Agathymus polingi S 0.668
Chiomara asychis* S 0.664
Pyrrhopyge araxes* S 0.654 λ
Agathymus mariae S 0.654
Atrytonopsis pittacus S 0.654
Codatractus arizonensis S 0.653 λ
Satyrium polingi S 0.652
Euphilotes rita W 0.65
Paramacera allyni S 0.646 λ
Callophrys fotis W 0.645
Chlosyne californica W 0.645 λ
Eurema dina* S 0.643
Eurema daira S 0.643
Phaeostrymon alcestis* E 0.641
Atrytonopsis lunus S 0.638 λ
Agathymus aryxna S 0.636
Eurema proterpia* S 0.636 λ
Kricogonia lyside S 0.632 λ
Euphyes bimacula E 0.631 λ
Calephelis wrighti W 0.628 λ
Agathymus stephensi S 0.627
Phyciodes batesii N 0.626
Atrytonopsis deva S 0.625
Atrytone arogos E 0.624 λ
Pyrgus xanthus W 0.623
Eurema boisduvaliana* S 0.623 λ
Callophrys henrici E 0.62
Microtia elva S 0.619
Gyrocheilus patrobas S 0.619
Euphilotes spaldingi W 0.618
Callophrys mcfarlandi W 0.618
Notamblyscirtes simius W 0.617 λ
Oarisma edwardsii* S 0.615 λ
Amblyscirtes oslari W 0.615 λ
Agathymus neumoegeni S 0.612
Megathymus ursus S 0.609

Figure 3

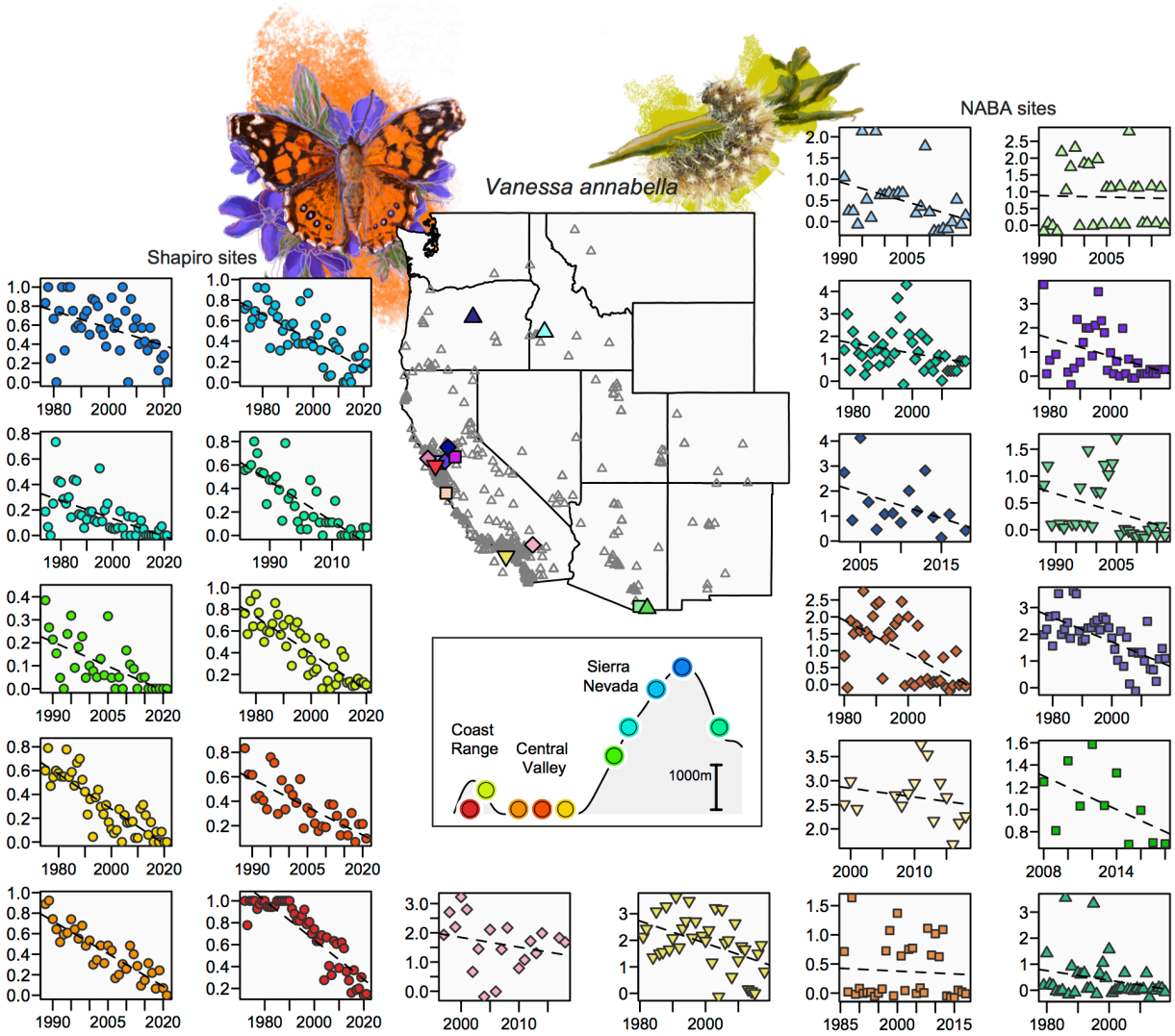
Vanessa annabella
Shapiro sites
NABA sites
Sierra Nevada
Coast Range
Central Valley
1000m

Figure 4

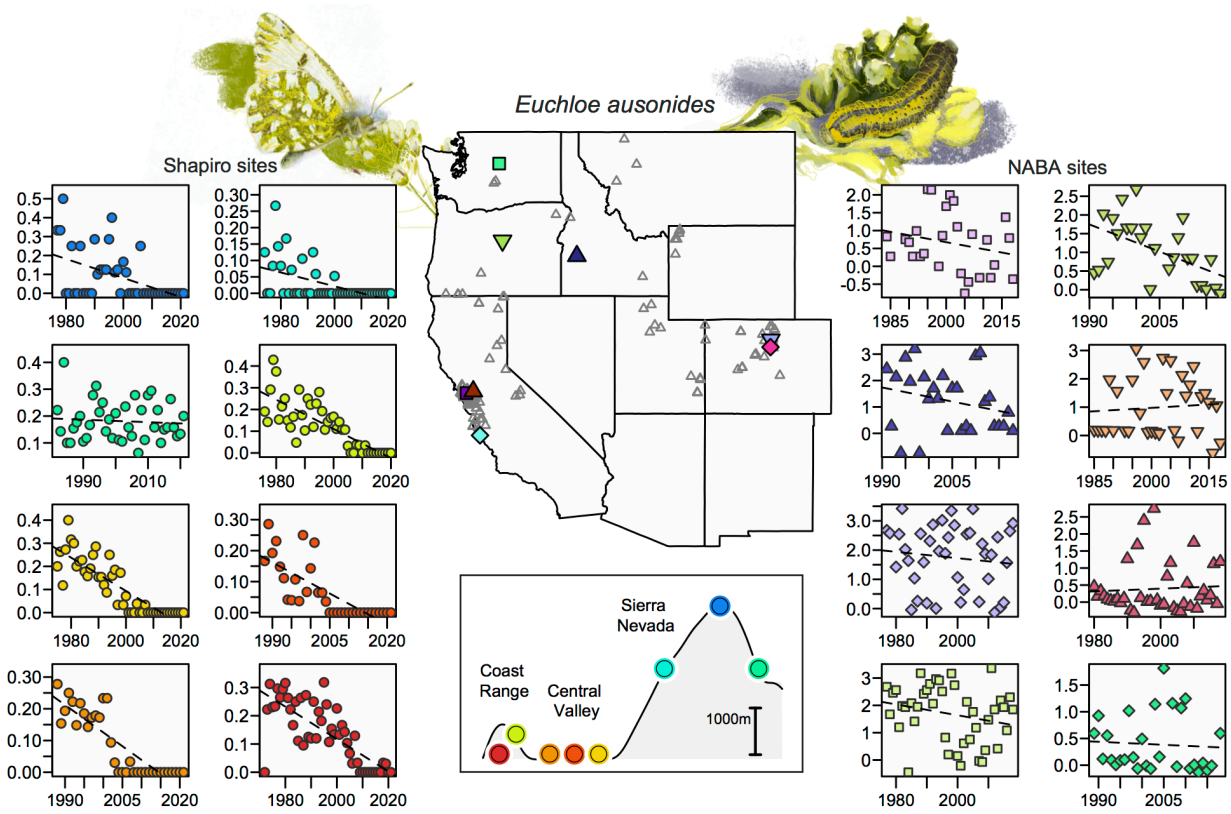
Euchloe ausonides
Shapiro sites
NABA sites
Sierra Nevada
Coast Range
Central Valley
1000m

Figure 5

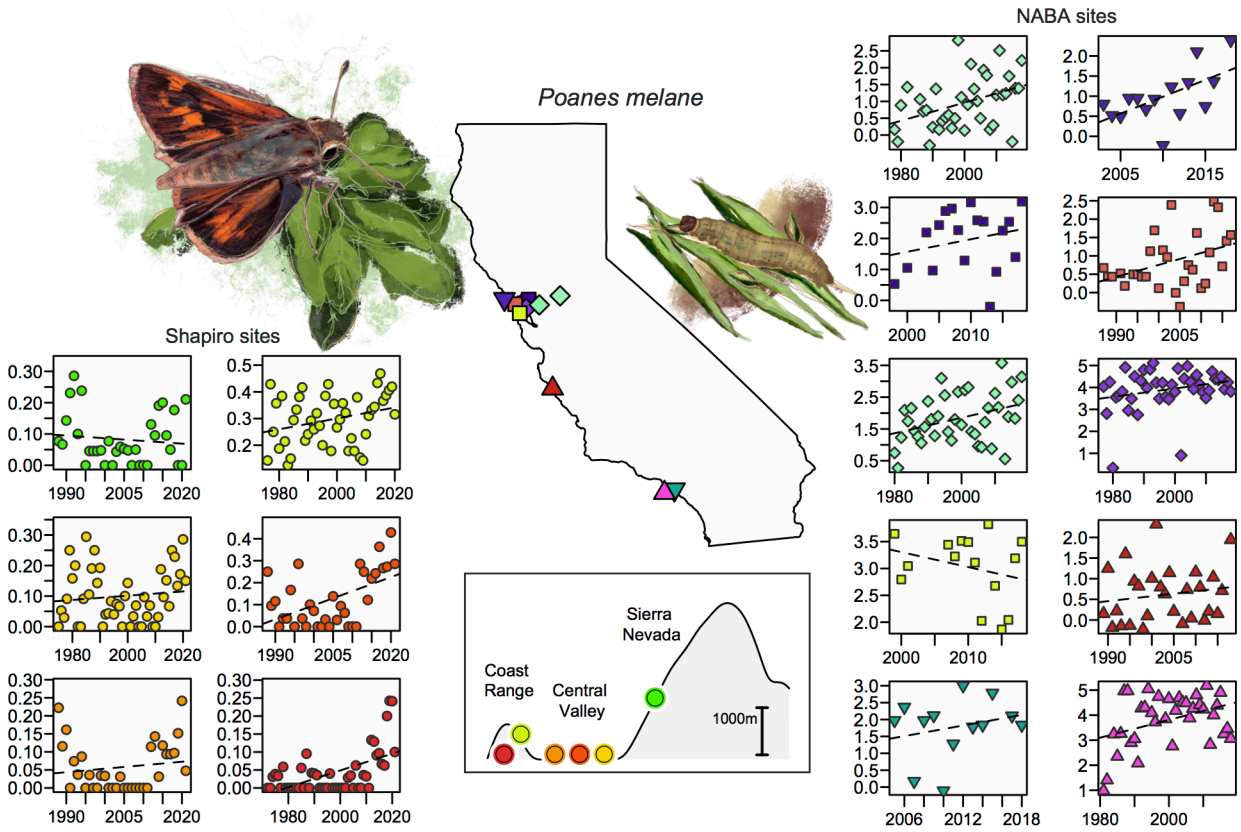
Poanes melane
Shapiro sites
NABA sites
Coast Range
Central Valley
Sierra Nevada
1000m

Figure 6

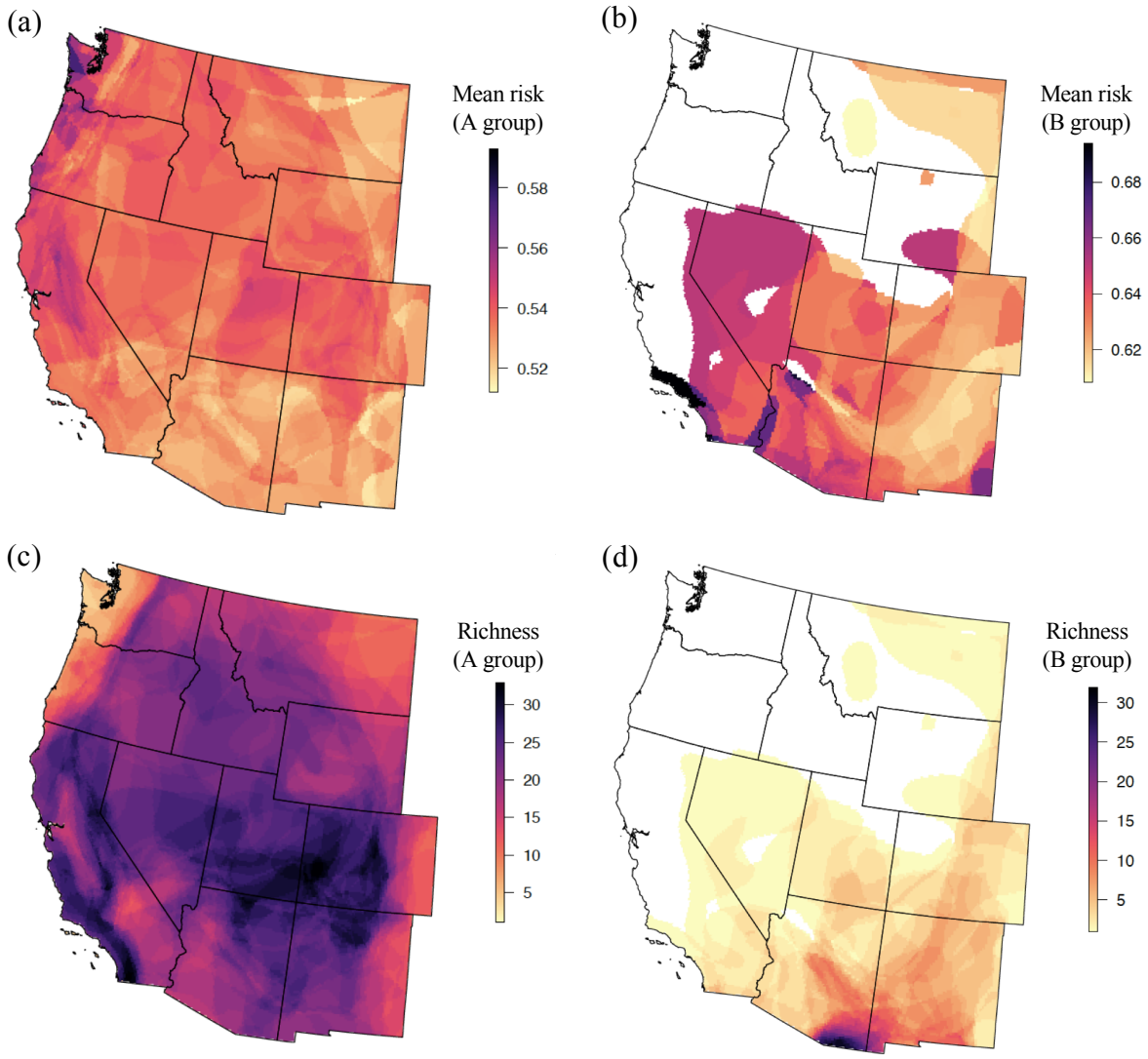
(a)
Mean risk
(A group)
0.58
0.56
0.54
0.52
(b)
Mean risk
(B group)
0.68
0.66
0.64
0.62
(c)
Richness
(A group)
30
25
20
15
10
5
(d)
Richness
(B group)
30
25
20
15
10
5

Figure 7

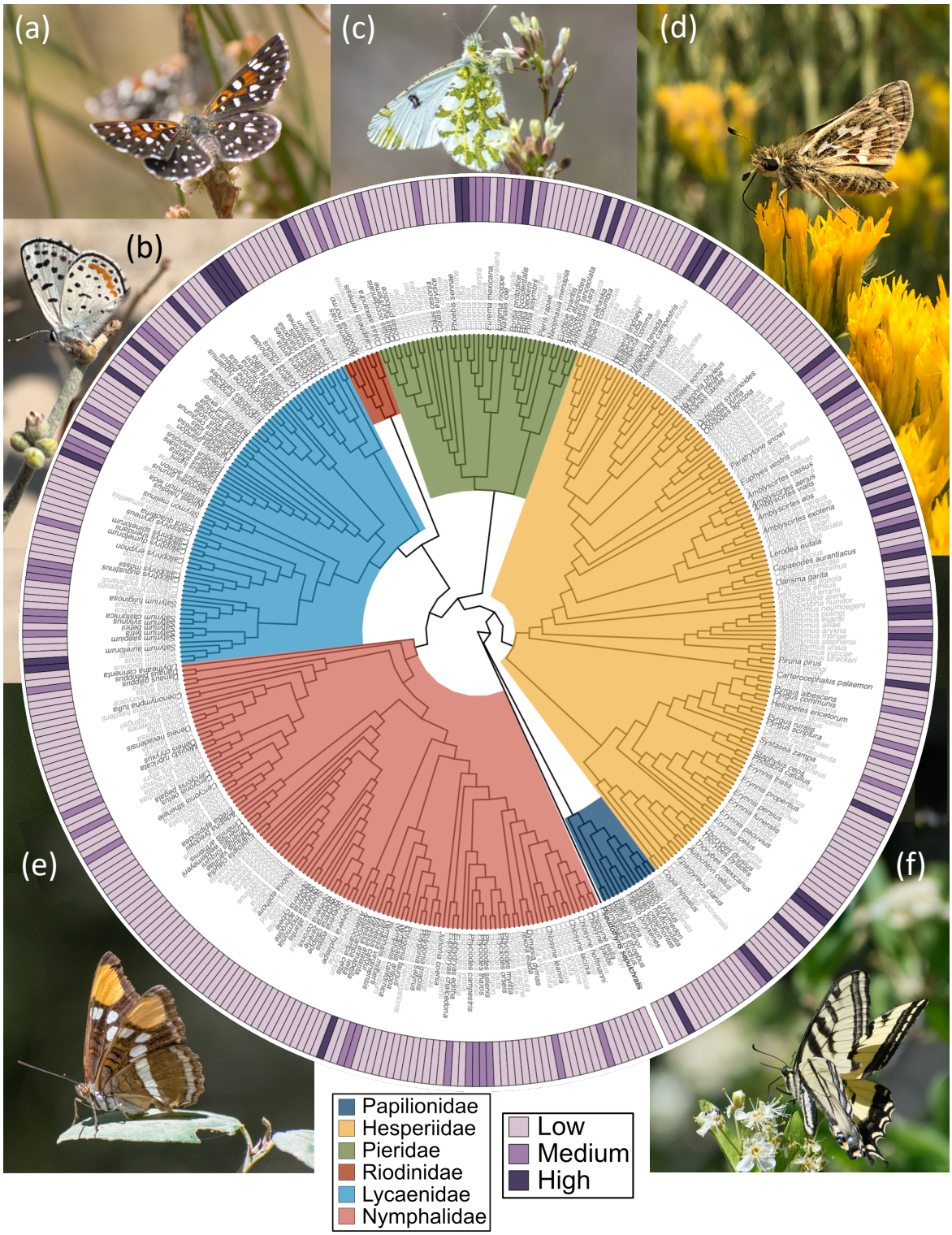
(a)
(b)
(c)
(d)
(e)
(f)
Papilionidae
Hesperiidae
Pieridae
Riodinidae
Lycaenidae
Nymphalidae
Low
Medium
High

Figure 8